Spatial Economics for Granular Settings*

Jonathan I. Dingel
Chicago Booth, NBER, and CEPR

Felix Tintelnot
University of Chicago, NBER, and CEPR

24 May 2020

Abstract

We introduce a general-equilibrium model of a "granular" spatial economy populated by a finite number of people. Our quantitative model is designed for application to the growing body of fine spatial data used to study economic outcomes for regions, cities, and neighborhoods. Conventional approaches invoking the law of large numbers are ill-suited for such empirical settings. We evaluate quantitative spatial models' out-of-sample predictions using event studies of large office openings in New York City. Our granular framework improves upon the conventional continuum-of-individuals model, which perfectly fits the pre-event data but produces predictions uncorrelated with the observed changes in commuting flows.

Keywords: commuting, granularity, gravity equation, quantitative spatial economics
JEL codes: C25, F16, R1, R13, R23

*We are grateful to Levi Crews and Mingjie Zhu for excellent research assistance. We thank Rodrigo Adão, Gabriel Ahlfeldt, Kirill Borusyak, Victor Couture, Teresa Fort, John Huizinga, Erik Hurst, Yuhei Miyauchi, Stephen Redding, Chris Severen, Daniel Sturm, and numerous conference and seminar participants for helpful feedback. Dingel thanks the James S. Kemper Foundation Faculty Research Fund at the University of Chicago Booth School of Business. This work was completed in part with resources provided by the University of Chicago Research Computing Center.
jdingel@chicagobooth.edu and tintelnot@uchicago.edu

1 Introduction

Economists increasingly use quantitative spatial models to evaluate urban policies such as infrastructure investments and land-use planning decisions. The growing availability of economic data observed at increasingly finer spatial scales offers tremendous potential for new insights. However, if policymakers are to rely on these models to inform their decision-making, researchers must establish that they reliably capture relevant features of the data and perform well in making counterfactual predictions (Bryan, Glaeser, and Tsivanidis, 2019, p.31).

Quantitative spatial models characterize spatial linkages by the gravity equation, which says that the volume of interactions between any two locations increases with their sizes and decreases with the bilateral frictions between them (Redding and Rossi-Hansberg, 2017). The gravity equation, in turn, is derived under the assumption that the volume of interactions between any two locations is large enough to wash out any idiosyncratic choices of individuals. But when locations are defined at fine spatial scales, the interactions between them are "granular." That is, individual decision-makers are large relative to the economic outcomes being analyzed. In such settings, the idiosyncratic choices of individual decision-makers do not wash out. By assuming a continuum of individuals, the extant literature has neglected granularity's influence on its counterfactual predictions.

In this paper, we introduce a new framework for the quantitative analysis of spatial linkages in granular settings. In doing so, we make four main contributions. First, we document that a number of empirical settings studied by economists feature commuting matrices that exhibit granularity. Second, we develop a quantitative spatial model that features a finite number of individuals and is suitable for counterfactual analysis. While incumbent models assume a continuum of individuals as a modeling convenience, our granular framework is just as tractable and matches the basic fact that no empirical setting has a continuum of individuals. Third, we show that estimates of commuting elasticities, workplace productivities, and residential characteristics can be very sensitive to how the granular features of the data are (implicitly) modeled. Fourth, we assess the "out-of-sample" predictions of quantitative spatial models using event studies of large changes in employment arising from new office openings. Regressing observed changes in commuting flows on the models' predicted changes shows that our granular model predicts these changes better than the conventional procedure applied to models assuming a continuum of commuters.

Section 2 shows that granularity is common in empirical settings of interest. Focusing on the United States, we examine tract-to-tract and county-to-county commuting matrices used in prior research. These settings are sufficiently granular that the commuting matrices are sparse: half or more of geographic pairs—within reasonable commuting distance—have zero commuters. We document that the commuter counts vary considerably from one year to the next, which may be a symptom of granularity. This impersistence poses a challenge for calibration methods that exactly replicate the commuting flows observed in a given year. Furthermore, commuting matrices' zeros are often asymmetric. As a result, calibration procedures that rationalize zero-commuter observations by infinite commuting costs impose severely asymmetric commuting costs despite the fact that daily commutes are round-trip journeys.

In Section 3, we propose a gravity-based general-equilibrium framework suitable for computing counterfactual outcomes in applications featuring granular commuting matrices. We follow the general-equilibrium approach employed in quantitative spatial models (e.g., Redding and Rossi-Hansberg 2017), but we assume that the number of individuals in the economy is finite. The key modeling challenge is that individual decisions affect wages and rents. We assume that individuals act as price takers and optimize given their beliefs about wages and rents. Employing standard discrete-choice methods (e.g., Train 2009), we model individuals choosing residence-workplace pairs on the basis of wage beliefs, rent beliefs, commuting costs, and an individual-specific idiosyncratic preference draw. We estimate the model assuming the price beliefs are "continuum-case rational expectations," which are the equilibrium prices in a model with the same parameters but a continuum of individuals. In our granular model, equilibrium outcomes depend in part on the idiosyncratic component of individuals' choices. Thus, where the continuum model would yield a single equilibrium allocation, our framework produces a *distribution* of economic outcomes instead. Notably, a single realization of the stochastic process often produces zeros for equilibrium outcomes that have strictly positive probabilities.

The continuum assumption has been made for reasons of convenience, not realism. Since our granular model is just as tractable as the continuum approach, it can be applied in the same empirical settings of interest. Moreover, since our granular framework coincides with the standard model in the limit, it can be used to quantify the role of granularity in economic outcomes and assess the (un)suitability of the continuum approximation.

Section 4 shows that the model's parameters can be estimated using the same data on commuting flows typically employed in the estimation of continuum-of-individuals models. Our maximum-likelihood estimator treats observed data as a realization from a multinomial count process. By contrast, the prior literature has frequently neglected the econometric concerns accompanying granularity. For example, the most common practice in the extant literature is to restrict the estimation sample to pairs of locations with strictly positive numbers of commuters between them. While discarding observations with zero commuters allows researchers to estimate the commuting elasticity using ordinary least squares, this practice has been criticized in the trade and industrial-organization literatures for introducing a selection bias (e.g., Eaton and Tamura 1994; Head and Mayer 2014; Wollmann 2018). The less common practice of recoding zeros as arbitrary small numbers introduces other biases. We find that these three estimation procedures deliver quite different parameter values in practice.

In Section 5, we describe how our framework can be used to compute counterfactual outcomes in granular empirical settings. Our framework's predictions about counterfactual outcomes can differ considerably from the conventional calibrated-shares procedure that equates observed shares and underlying probabilities. We illustrate that the calibrated-shares procedure predicts land-price changes in response to a productivity increase that are, quantitatively, very close to proportional to incumbent workers' residential shares prior to the counterfactual change. The granularity and impersistence of commuting flows suggest that these predictions are likely an artifact of overfitting

the model to the observed data. By contrast, our granular framework ties the incidence of the productivity improvement on local land prices to observable commuting frictions between residential locations and the workplace, such as distance or commuting time, and predicts a distribution of counterfactual outcomes.

We assess quantitative spatial models' suitability for counterfactual analysis by comparing their predictions for changes in commuting flows to observed outcomes after a local economic shock. Examining the "out-of-sample" performance of these models is an important step in establishing their value as an input into urban planning and other policymaking decisions. We examine commuting flows, which are consistently reported in available data and the key spatial linkage between neighborhoods in many models of cities. We study events in which there is a large, discrete increase in employment in a single census tract arising from the arrival of a large employer such as Google or Tiffany & Co. We increase the productivity parameter for that tract to match the increase in total employment and compare the predicted changes in bilateral commuting flows to those observed in the data. When examining 78 events of tract-level employment booms in New York City, we find that our granular framework predicts the observed changes in commuting flows better than the calibrated-shares procedure for 76 of these events. While predictive performance varies across events, regressing the observed change in commuters on the granular model's prediction typically yields an estimated slope of one, whereas the estimated slope for the calibrated-shares procedure is often near zero or negative. In other words, the counterfactual predictions from the calibrated-shares procedure are *negatively* correlated with the observed changes in commuting in more than half of the 78 events.

At first glance, it may be surprising that our granular model predicts changes in commuter counts better than the procedure that calibrates parameters to perfectly fit the pre-event flows. For intuition, note that each observation in the pre-event cross section has three parts: a time-invariant component correlated with included covariates, a time-invariant component uncorrelated with those covariates, and a time-varying component. On the one hand, the advantage of the calibrated-shares procedure is its potential to capture real spatial linkages not predicted by covariates like transit times, such as the fact that a very large share of Columbia University employees reside in nearby university-owned residences. On the other hand, the calibrated-shares procedure matches every bit of variation in the data, including transitory individual idiosyncrasies. This risks overfitting the third component of the pre-event observations and failing to predict post-event outcomes. In our event studies, the overfitting problem dominates. We explore the extent to which pooling several years of pre-event data can improve the models' predictions. While pooling improves the calibrated-shares procedure's predictions such that they are positively correlated with the observed changes in almost two-thirds of the events, the granular model still outperforms the calibrated-shares procedure in 65 of 78 events.

We contribute to the rapidly expanding literature on quantitative spatial economics.[1] A growing

[1] In gravity-based quantitative models, a location's access to all other locations' goods and factors, which is impeded by bilateral frictions, influences the magnitude and character of its economic activity. See Proost and Thisse (2019) for a recent survey of these models, Donaldson (2015) on market access in goods trade, Redding and Turner (2015)

body of research aims "to provide an empirically relevant quantitative model to perform general equilibrium counterfactual policy exercises" concerning topics such as transportation-infrastructure investment, neighborhood revitalization programs, and local business tax incentives (Redding and Rossi-Hansberg, 2017, p.23).[2] As anticipated by Holmes and Sieg (2015, p.106), "[a]s research in urban and regional applications takes advantage of new data sets at high levels of geographic resolution, it permits the study of interactions at narrow levels, where there may be relatively few decision-makers," but quantitative spatial models have largely abstracted from discreteness in the underlying economic environment. The extant literature takes two distinct approaches when applying a continuum model to residence-workplace pairs with zero commuters, which are the most obvious symptom of granularity. The calibrated-shares procedure rationalizes zeros by imposing infinite commuting costs or disamenities, so that every residence-workplace pair with zero commuters in the observed equilibrium has zero commuters in any counterfactual scenario.[3] The second approach makes bilateral commuting costs a function of observable (or computed) transit times that take finite values and therefore cannot produce the zero-commuter outcomes that are pervasive in the data.[4] Our granular framework generates zeros without imposing infinite costs.

Our event studies of new office openings contribute to a much smaller literature assessing the predictive power of quantitative spatial models using observed economic changes. Ahlfeldt et al. (2015) demonstrate their quantitative model's ability to capture how changes in floor prices associated with Berlin's division and reunification correlated with distance to the pre-war central business district. Monte, Redding, and Rossi-Hansberg (2018) verify a qualitative implication of their quantitative spatial model—larger employment responses to a local productivity increase in counties more open to commuting—using the million-dollar-plant openings examined by Greenstone, Hornbeck, and Moretti (2010). Adão, Arkolakis, and Esposito (2020) compare US commuting zones' actual and predicted changes in employment and wages in response to the "China shock" of Autor, Dorn, and Hanson (2013) for different calibrations of spatial links. Kreindler and Miyauchi (2020) use a gravity model and cell-phone–derived commuting flows to predict workplace wage levels in developing-economy cities that lack conventional data coverage. We explore the consequences of the widespread continuum assumption for the predictive power of quantitative spatial models in granular settings.

on transport costs for both goods and commuters, and Dingel (2017) on the income composition of goods market access.

[2] Heblich, Redding, and Sturm (2018); Severen (2019); Tsivanidis (2019); and Zárate (2019) study transportation-infrastructure investments. Owens, Rossi-Hansberg, and Sarte (2020) evaluate strategic visions to revitalize Detroit. Berkes and Gaetani (2020) compare the effects of siting Amazon's HQ2 in four different New York City neighborhoods.

[3] Heblich, Redding, and Sturm (2018, p.22) and Monte, Redding, and Rossi-Hansberg (2018, p.3869) both write that the "model implies prohibitive commuting costs" for all "pairs with zero commuting flows." In a panel setting, Severen (2019) imposes prohibitive commuting costs for tract pairs that had zero commuters in both time periods when computing counterfactual outcomes.

[4] See, for example, Ahlfeldt et al. (2015), Allen, Arkolakis, and Li (2015), and Tsivanidis (2019). Ahlfeldt et al. (2015) and Tsivanidis (2019) analyze commuting data reported at a coarser level of aggregation than the geographic units they study. Making bilateral frictions a function of observed characteristics allows them to estimate commuting elasticities using aggregated data but apply their models to (unobserved) commuting between smaller geographic units.

Finally, our framework is also related to research about granular economies and discrete-choice estimation. A growing literature examines the importance of granularity for aggregate fluctuations in macroeconomics (Gabaix, 2011; Carvalho and Grassi, 2019) and international economics (di Giovanni and Levchenko, 2012; di Giovanni, Levchenko, and Mejean, 2014; Gaubert and Itskhoki, 2018; Daruich, Easterly, and Reshef, 2019). In addition to its relevance for aggregate fluctuations, firm-level granularity has been studied as one explanation for zeros in the international trade matrix (Eaton, Kortum, and Sotelo, 2013; Armenter and Koren, 2014).[5] Recent research in industrial organization draws attention to the problems associated with zero-valued market shares (Quan and Williams, 2018; Gandhi, Lu, and Shi, 2019; Dubé, Hortaçsu, and Joo, 2020). Mogstad et al. (2020) raise concerns about inference for ranks in granular settings. Our paper makes two contributions to these various strands of the literature. First, we provide a general-equilibrium modeling approach to granularity, namely continuum-case rational expectations, that is easy for practitioners to implement. Second, we demonstrate the importance of addressing granularity when making predictions about counterfactual outcomes.

2 Granular empirical settings

This section documents that granularity is common in empirical settings in which researchers and policymakers are interested in the incidence of local economic shocks. We primarily focus on the United States, examining tract-to-tract and county-to-county commuting matrices. After establishing that these settings are granular, we document two additional patterns that are likely symptoms of granularity: the commuter counts are impersistent over time, and zeros in the matrices are often asymmetric.

2.1 Data sources

We employ commuting matrices at two different spatial scales for the United States. First, we use data on commuting between census tracts taken from the Longitudinal Employer-Household Dynamics, Origin-Destination Employment Statistics (LODES). For illustrative purposes, we restrict our attention to pairs of tracts in the Detroit urban area and New York City.[6] Second, we use data on commuting between US counties taken from the American Community Survey (ACS), which surveys roughly 5% of the US population over a five-year period.[7]

An immediate implication of granularity is that some data providers perturb observations to protect confidentiality. For example, the published LODES tract-level workplace employment

[5] Alternatively, one may generate zeros when there is a continuum of firms by assuming fixed costs and a bounded productivity distribution, as in Helpman, Melitz, and Rubinstein (2008).

[6] Owens, Rossi-Hansberg, and Sarte (2020) use the 2014 wave of these data for the Detroit urban area to estimate a gravity model of commuting. Davis et al. (2019) use the 2010 wave to compute the joint distribution of residences and workplaces for New York City. Following Owens, Rossi-Hansberg, and Sarte (2020), we use the primary-job counts in LODES.

[7] Monte, Redding, and Rossi-Hansberg (2018) use the 2006–2010 wave of this survey to estimate a gravity model of commuting.

counts are noise-infused. Moreover, the published LODES commuting matrices report synthetically generated residence-workplace pairs.[8] These confidentiality-protecting procedures are both a symptom of the granular setting and an additional cause for caution when interpreting the value of any individual observation.[9]

2.2 Tract-to-tract commuting matrices are granular

When working with fine spatial units like US census tracts, simply comparing the number of people and the number of residence-workplace pairs reveals that the empirical setting is granular. For example, the Detroit urban area has about 1.3 million pairs of census tracts and about 1.3 million commuters. Thus, the average cell in the commuting matrix contains one person. As 74% of tract pairs have zero commuters between them, the average positive cell contains about four people. As shown in the left panel of Figure 1, nearly half of the tract pairs with a positive number of commuters have only one commuter. More than 12% of Detroit commuters are the sole commuter in their cell of the commuting matrix. For such observations, a change in one individual's choice alters the commuting flow by 100%. The right panel of Figure 1 shows similar patterns in New York City.[10]

Figure 1: Number of commuters between pairs of tracts in Detroit and New York City

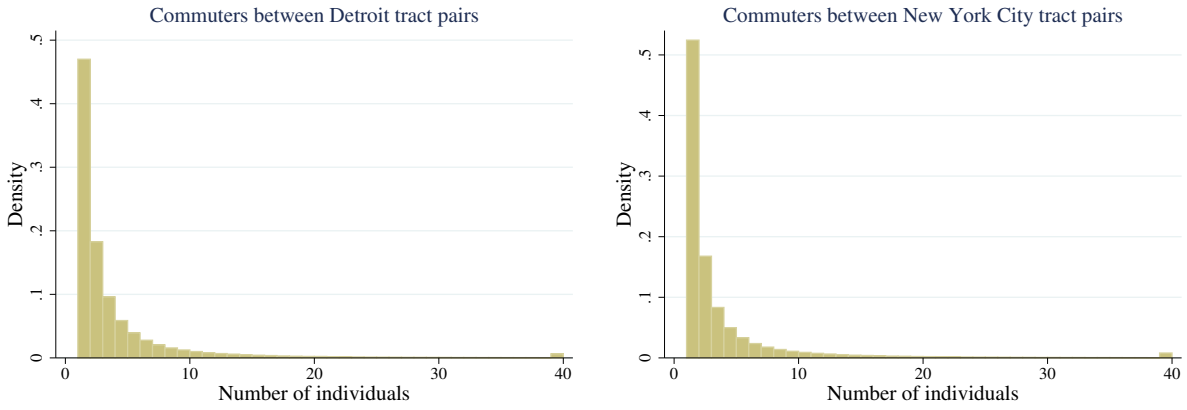

NOTES: These histograms report the number of tract pairs in the Detroit urban area (left panel) and New York City (right panel) by the number of individuals who reside in the origin tract and work in the destination tract in 2014 LODES data. These histograms restrict the samples to pairs of tracts with a strictly positive number of commuters. There are 1166 residential census tracts in Detroit. There are 2168 residential census tracts in New York City.

[8] Graham, Kutzbach, and McKenzie (2014): "For each job in a workplace cell, LODES draws from a Dirichlet multinomial posterior distribution of possible residential locations... The prior adds uncertainty, so that even commutes with few or no observed flows may appear to have a job. Conversely, even when there are commuters from an origin in the likelihood, that residence may not be drawn and thus would not appear in LODES."

[9] The econometric consequences of noise infusion and synthetic observations are specific to each use case. For example, see the discussion of these issues in Couture and Handbury (2019). Calibration approaches that perfectly match every (synthetic) observation are likely the research design most sensitive to these procedures.

[10] About 2.5 million of New York City's 8 million residents are employed in New York City. Since New York City's commuting matrix has more than 4.6 million cells, its average cell contains slightly more than half a commuter, and this matrix is almost necessarily sparse.

In fact, commuting matrices describing tract-to-tract flows for large US cities are inherently granular. Tracts are defined by the US Census Bureau such that the typical tract has 4,000 residents.[11] Thus, both the number of commuters and the number of tracts are roughly proportionate to the city's residential population, and the mean value of a cell in the tract-to-tract commuting matrix is inversely proportionate to that population.[12] In metropolitan areas with million of residents, the mean cell value is about one commuter. Since commuting flows take integer values, smaller mean values of cells make the commuting matrix necessarily granular and possibly even sparse.[13]

The spatial concentration of employment contributes to the sparsity of commuting matrices in settings with small spatial units. When these small spatial units are defined by street blocks or residential counts, the concentration of employment (relative to residences) implies that many workplace destinations have a smaller number of employees than the number of residential origins. The Detroit urban area illustrates the consequence. The median tract in the Detroit urban area has 465 employees working in it. Since Detroit has 1,166 residential tracts, at least 60% of locations must have zero residents commuting to this workplace.

Urban economists have studied other empirical settings in which the fine spatial resolution of the geographic units employed makes the commuting matrix necessarily granular. Roughly three-quarters of the cells in the Los Angeles metropolitan commuting matrix studied by Severen (2019) are empty.[14] Tsivanidis (2019) models the behavior of Bogota's 8 million residents commuting between almost 7 million pairs of tracts. Zárate (2019) examines Mexico City, which has 9 million people commuting between 13 million pairs of tracts. Ahlfeldt et al. (2015) model the behavior of about 3 million Berliners choosing among nearly 254 million pairs of city blocks.

2.3 The US county-to-county commuting matrix is granular

The commuting matrix for US counties is granular despite the large number of people relative to the number of county pairs. In the 2006–2010 ACS data, there are 136 million commuters (with commutes less than 120 kilometers).[15] Of those 136 million, 101 million live and work in the same county, so there are 35 million cross-county commuters between 79,188 pairs of counties. Thus, the average off-diagonal element of the county-to-county commuting matrix has 445 commuters. However, the distribution of commuters is extremely uneven. The top 10 county pairs account for more than 2 million commuters alone. For the bottom 90% of off-diagonal observations, the mean value is only 40 commuters. Figure 2 shows that this distribution is skewed, so that many

[11] Geography Program glossary: "Census tracts generally have a population size between 1,200 and 8,000 people, with an optimum size of 4,000 people."

[12] To be more precise, in a city with R residents and I workers, there are about $N \approx R/4000$ tracts, and the mean value of each commuting cell in a tract-to-tract matrix is approximately $\frac{I}{N^2} = \frac{I}{R}\frac{16 \text{ million}}{R}$.

[13] The typical employed resident has only one place of employment. This imposes an integer constraint on commuting flows not relevant for trade flows or transaction flows, since firms can export to multiple destinations and shoppers can patronize multiple businesses.

[14] Comparing Tables 2 and F4 of Severen (2019) shows that each column of the latter has about four times as many observations as its counterpart in the former.

[15] We follow Monte, Redding, and Rossi-Hansberg (2018) by restricting attention to county pairs that are less than 120 kilometers apart.

thousands of county pairs have small numbers of commuters.

Figure 2: Number of commuters between US counties

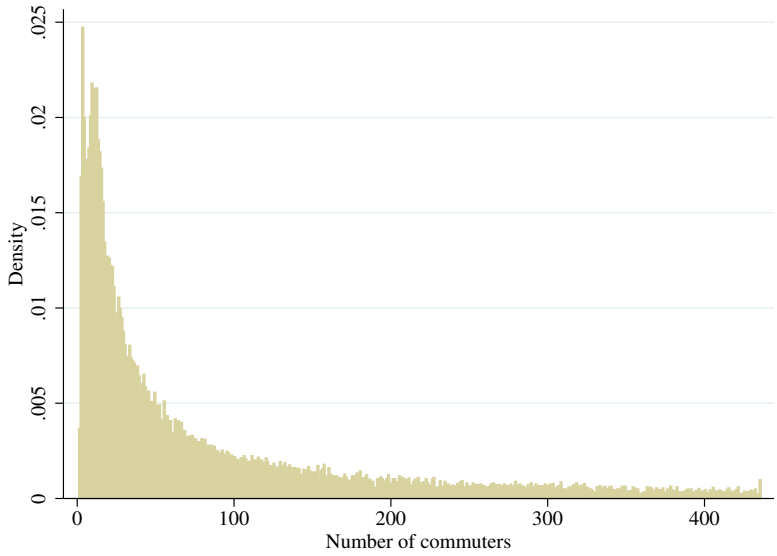

NOTES: This histogram depicts the number of county pairs by the estimated number of commuters in the 2006–2010 ACS. The sample is restricted to pairs of distinct counties within 120 kilometers, the smallest 90% of estimated commuter counts among such counties, and only those pairs reporting a strictly positive number of commuters.

In practice, the granularity of this empirical settings is severely compounded by the fact that the ACS is a 1-in-20 sample of the population. In three different five-year waves of the ACS, nearly half of the county pairs within 120 kilometers of each other are reported to have zero commuters, as shown in Table 1. More than half of county pairs report fewer than 100 commuters, therefore representing the behavior of five or fewer respondents. As a consequence, as shown in the third column of Table 1, for more than one-third of the county pairs with positive commuting flows, the Census-reported margin of error exceeds the reported number of commuters.[16]

Commuting data from other countries also exhibit granularity. For example, one-quarter of Germany's county (Kreisfreie Städte and Landkreise) pairs within 120 kilometers have fewer than 10 commuters (Krebs and Pflüger, 2019). In Brazil's 2010 Censo Demográfico, which reports estimates based on a 10% sample of the population, there are 81 million commuters (with commutes less than 60 kilometers).[17] There are 7 million cross-municipality commuters between 131,620 pairs of municipalities. Thus, the average off-diagonal element of the municipality-to-municipality commuting matrix has only 56 commuters. About three-quarters of the cells in this commuting matrix are empty.

[16] At face value, this would seem to imply that one could not reject the null hypothesis that there were no commuters for such county pairs. The unsuitability of the normal approximation for the binomial distribution in this case is another symptom of granularity.

[17] Dingel, Miscio, and Davis (2019) use these data to construct metropolitan areas based on commuting flows.

Table 1: Zeros in US county-to-county commuting matrix

Dataset	Zero Pairs	Positive Pairs	MOE >X (percent)
ACS 2006-2010	36,403	42,785	37
ACS 2009-2013	35,547	43,641	36
ACS 2011-2015	35,002	44,096	35

NOTES: This table reports the number of county pairs with zero commuters and non-zero commuters for three editions of the ACS. The sample is restricted to pairs of counties within 120 kilometers of each other. The final column reports the share of county pairs for which the Census-reported margin of error exceeds the (strictly positive) reported number of commuters.

2.4 Commuting counts are often impersistent

We now describe the first of two patterns that are likely symptoms of granularity. The integer values appearing in commuting matrices are not very persistent. A residence-workplace pair may have three commuters one year and none the next. Another pair of locations may double its number of commuters, from one to two. While the conventional continuum approach interprets these changes as substantial economic shifts, the finite-sample perspective is that these changes are not very informative if they are merely a symptom of granularity. We document substantial churn in commuting counts from year to year, suggesting that there is considerable finite-sample noise in addition to signal in these commuting counts.

Table 2, which presents the transition matrix for pairs of tracts in the Detroit urban area between the years 2013 and 2014, demonstrates considerable impersistence. For pairs with one to four commuters in 2013, the percentages appearing on the diagonal of the transition matrix are quite low. A pair of tracts with one commuter in 2013 was almost three times as likely to have zero commuters in 2014 than to have one commuter. A pair with four commuters in 2013 was more likely to appear in any other column in 2014 than to report four commuters again. The 86% of pairs that had zero commuters in both years may appear to suggest persistence, but this primarily is a symptom of the fact that in both years about three-quarters of observations are zero.[18] More than 130,000 pairs of tracts that had zero commuters in 2013 had at least one commuter in 2014. At the same time, 39% of Detroit tract pairs with positive flow in 2013 were zeros in 2014 . Thus, while zeros are pervasive in this commuting matrix, they are not very persistent. The results for New York City in Table 2 are very similar to those for Detroit. The commuter counts are so impersistent that, for many tract pairs, a gravity-based estimate predicts a tract-pair's commuter count in 2014 better than its observed count in 2013 does, as reported in Appendix A.

There is considerable churn even when using larger geographic units. Table 3 shows that 22% of the county pairs reporting zero commuters in the 2006–2010 ACS reported a positive number of

[18] If $p \in [0, 1]$ of the pairs were randomly independently assigned zero in each period, then p^2 of those pairs would lie in the upper left cell of the transition matrix. Thus, even if zeros were randomly independently assigned to three-quarters of tract pairs in each period, nine-sixteenths of the pairs would be zero in both periods. That would not be evidence of persistence.

Table 2: The impersistence of commuting counts for pairs of tracts in Detroit and New York City

(a) Detroit

	2014					
2013	0	1	2	3	4	5+
0	0.86	0.10	0.02	0.01	0.00	0.00
1	0.60	0.22	0.10	0.04	0.02	0.02
2	0.37	0.25	0.16	0.09	0.06	0.08
3	0.23	0.22	0.18	0.13	0.08	0.16
4	0.15	0.17	0.17	0.14	0.11	0.26
5+	0.04	0.06	0.07	0.08	0.08	0.68

(b) NYC

	2014					
2013	0	1	2	3	4	5+
0	0.91	0.07	0.01	0.00	0.00	0.00
1	0.65	0.20	0.08	0.04	0.02	0.02
2	0.39	0.25	0.15	0.09	0.05	0.07
3	0.24	0.22	0.17	0.12	0.08	0.16
4	0.15	0.17	0.17	0.14	0.11	0.27
5+	0.03	0.05	0.06	0.07	0.07	0.71

NOTES: This table describes pairs of tracts in the Detroit urban area (left panel) and New York City (right panel) by reported number of commuters in the 2013 and 2014 LODES. It is a transition matrix, in which each cell lists the share of tract pairs in that row (number of commuters in 2013) that belong to that column (number of commuters in 2014). Each row sums to 100%, modulo rounding.

commuters in the following five-year interval. Conversely, about 15% of pairs reporting a positive number of commuters had zero commuters in the following five-year interval. For pairs of counties with a strictly positive number of commuters smaller than 111 in 2006–2011, the diagonal elements of the transition matrix are less than half. For example, a pair of counties reported to have 71–90 commuters in 2006–2011 has only a 14% probability of appearing in the same bin in the following five-year interval.

To the extent that the observed impersistence of commuting counts is a symptom of granularity, these findings caution against procedures that infer structural parameters from the relative magnitudes of these counts. The difference between one commuter and two commuters (or one respondent and two respondents in a finite sample) is little evidence that the latter outcome was twice as probable. Similarly, procedures that rationalize observations with zero commuters by imposing infinite commuting costs so that these are zero-probability events rule out potential margins of adjustment based on zeros that appear to be largely transitory.

2.5 Zeros are often asymmetric

The zeros in commuting matrices are often asymmetric. Denoting the number of commuters living in residence k and working in workplace n by ℓ_{kn}, an observed zero is asymmetric when $\ell_{nk} = 0$ and $\ell_{kn} > 0$. For US counties, $\ell_{nk} = 0$ for 22% of county pairs with $\ell_{kn} > 0$. In Detroit, $\ell_{nk} = 0$ for 66% of tract pairs with $\ell_{kn} > 0$. For Brazilian municipalities, $\ell_{nk} = 0$ for 49% of municipio pairs with $\ell_{kn} > 0$. These asymmetric flows are not explained by asymmetric numbers of total employees or residents: in Detroit, $\ell_{nk} = 0$ for 47% of tract pairs for which $\ell_{kn} > 0$ and total employment in k and n differs by 10% or less.

The fact that commuting matrices' zeros are often asymmetric poses a puzzle for calibration procedures that rationalize zero-commuter observations by infinite commuting costs. This interpretation of zeros implies severely asymmetric commuting costs, even though daily commutes are

Table 3: The impersistence of commuting counts for pairs of US counties

2006-2010 \ 2011-2015	Initial Share(%)	0	1-30	31-50	51-70	71-90	91-110	111-500	501-1,500	>1,500
0	45.97	0.78	0.18	0.02	0.01	0.00	0.00	0.00	0.00	0.00
1-30	19.66	0.35	0.45	0.10	0.05	0.02	0.01	0.02	0.00	0.00
31-50	5.47	0.16	0.36	0.19	0.12	0.07	0.04	0.07	0.00	0.00
51-70	3.43	0.08	0.26	0.18	0.15	0.10	0.08	0.15	0.00	0.00
71-90	2.50	0.05	0.16	0.15	0.16	0.14	0.12	0.23	0.00	0.00
91-110	1.86	0.02	0.11	0.12	0.15	0.12	0.13	0.35	0.00	0.00
111-500	12.03	0.00	0.02	0.03	0.04	0.05	0.05	0.74	0.07	0.00
501-1,500	5.01	0.00	0.00	0.00	0.00	0.00	0.00	0.13	0.81	0.06
>1,500	4.07	0.00	0.00	0.00	0.00	0.00	0.00	0.00	0.06	0.94

NOTES: This table presents a transition matrix for pairs of counties within 120 kilometers of each other by reported number of commuters in two editions of the ACS. The first column reports the percentage of county pairs that were in each row in the 2006–2010 data. The remaining columns report the share of county pairs within the row that appeared in the corresponding bin in the 2011–2015 data. By definition, the shaded cells in each row sum to one, modulo rounding. The bin boundaries are arbitrary, since Figure 2 shows no obvious bunching. We found similar impersistence when using alternative boundaries.

roundtrip journeys. If we believe that commuting from n to k is impossible because we observe $\ell_{nk} = 0$, how do the individuals who live in k and work in n commute home at the end of the day? The mechanisms generating prohibitive commuting costs would have to exhibit within-day variation. But the most plausible source of intraday variation in commuting costs — congestion caused by a large number of commuters — cannot explain residence-workplace pairs that have no commuters.

In many empirical settings, asymmetric zeros may simply be a symptom of granularity rather than evidence of very asymmetric commuting costs. When most pairs of locations have zero commuters, and the modal pair with a positive number reflects the decision of only one commuter or one survey respondent, the difference between zero and one isn't particularly informative.

3 Model

This section introduces a model of granular residential and workplace location choices. We combine tools used to describe a finite number of individuals' decisions employed in the discrete-choice literature (e.g., Train 2009) with the general-equilibrium approach employed in quantitative spatial models (e.g., Redding and Rossi-Hansberg 2017). Extensions of the core model that introduce trade costs, local increasing returns, and production employing land are presented in Appendix B.

The key challenge in modeling a finite number of people is that individual decisions can affect wages and rents. This raises two issues. First, do individuals internalize the effects of their own choices on local labor supplies and land demands? Second, are individuals able to enumerate the

prices induced by every possible combination of others' choices? In the interest of tractability, we assume that individuals have common point-mass beliefs about wages and rents. Therefore, individuals act as price takers, as in the granular economy of Gabaix (2011). In practice, we assume that these beliefs are "continuum-case rational expectations." In other words, given the model parameters, each individual forms their beliefs about wages and rents using the conventional continuum model, which is a limit case of our model as the number of individuals goes to infinity.

3.1 Setup

We consider a closed economy populated by I individuals. There is a set of locations indexed by k or n. Each location k is endowed with a quantity of land, T_k, that is owned by immobile landlords who consume only goods.[19] Each location is endowed with the technology to produce a differentiated good (i.e., the Armington assumption). For simplicity, we abstract from trade costs.

Individuals (denoted by i) have Cobb-Douglas preferences over these traded goods and land, devoting α of their expenditure to the latter. They have constant elasticity of substitution (CES) preferences over the set of differentiated goods, with elasticity of substitution $\sigma > 1$. Individuals have idiosyncratic tastes for pairs of residential and workplace locations, such that i's indirect utility from living in k and working in n is

$$U_{kn}^i = \underbrace{\epsilon \ln\left(\frac{w_n}{\Phi_k \delta_{kn}}\right)}_{\equiv U_{kn}} + \nu_{kn}^i, \tag{1}$$

where w_n denotes the wage in location n, Φ_k denotes the price index of location k, $\delta_{kn} \geq 1$ denotes the commuting cost between k and n, U_{kn} denotes the mean utility of choice kn, and ν_{kn}^i is the idiosyncratic utility draw of individual i for living in k and working in n. The parameter ϵ governs the importance of mean utility relative to the idiosyncratic utility draw. Given Cobb-Douglas preferences, the price index in location k is $\Phi_k = r_k^\alpha P^{1-\alpha}$, where r_k denotes the local land price, and P denotes the common CES price index for goods. We assume that ν_{kn}^i is drawn from a type 1 extreme value distribution.

Production of each location's differentiated good is linear in labor. The goods market is perfectly competitive.[20] Each individual is endowed with L/I units of labor, such that the aggregate labor endowment is L. Commuting is costly because time spent commuting is not spent working, so that individuals residing in k and working in n earn only w_n/δ_{kn} because they only spend $1/\delta_{kn}$ of their time working.[21] Workers produce in location n with a linear production technology: $q_n = A_n L_n$, where L_n is the quantity of labor supplied by workers working in n and A_n is that location's productivity. Given this production function and perfect competition, the price of location n's

[19] This simplifying assumption follows Monte, Redding, and Rossi-Hansberg (2018).

[20] Given established isomorphisms between perfect-competition and monopolistic-competition models of economic geography (e.g., Allen and Arkolakis 2014), this assumption is not crucial to our results. See discussion in Appendix B.

[21] Alternatively, we could assume that δ_{kn} represents a utility shifter that does not affect working time. Modeling δ_{kn} as reduced working time facilitates the commuting-elasticity estimation discussed in Section 4.

output is w_n/A_n for all consumers. Thus, the CES price index is $P = \left[\sum_n (w_n/A_n)^{1-\sigma}\right]^{1/(1-\sigma)}$.

We make the following assumptions about information and expectations. All workers know the primitives of the model (L, $\{A_n\}$, $\{T_k\}$, $\{\delta_{kn}\}$, α, ϵ, σ) and have (common) expectations about the equilibrium variables r_k and w_n. We assume that the price expectations are point-mass beliefs, such that each individual assigns 100% probability to a single vector of wages and a single vector of land prices. Denote these belief vectors by $\{\tilde{w}_n\}$ and $\{\tilde{r}_k\}$. Worker i knows her idiosyncratic preferences $\{\nu^i_{kn}\}$.

Decisions are made and markets clear in the following order. Based on beliefs $\{\tilde{w}_n\}$ and $\{\tilde{r}_k\}$, each worker chooses the residential location and the work location that maximize expected utility

$$\tilde{U}^i_{kn} = \underbrace{\epsilon \ln\left(\frac{\tilde{w}_n}{\tilde{P}^{1-\alpha}\tilde{r}_k^{\alpha}\delta_{kn}}\right)}_{\equiv \tilde{U}_{kn}} + \nu^i_{kn}, \tag{2}$$

where $\tilde{P} = \left[\sum_n (\tilde{w}_n/A_n)^{1-\sigma}\right]^{1/(1-\sigma)}$. After these decisions are made, workers are immobile and cannot relocate. Realized equilibrium land prices r_k and wages w_n are those that clear goods, labor, and land markets given individuals' residential and workplace locations.

The assumption that individuals have point-mass beliefs about wages, $\{\tilde{w}_n\}$, and rents, $\{\tilde{r}_k\}$, considerably simplifies the analysis. Otherwise, individuals would need to compute the prices associated with all possible residence-workplace allocations and then solve for the fixed-point probabilities that each of these occurs. The set of feasible allocations is large. For example, a granular economy with only 10 individuals and 16 workplace-residence pairs would have more than 3 million possible allocations.[22] For empirically relevant magnitudes, computing the number of possible allocations leads to such large numbers that they cause overflow problems in standard software. While our approach is general in the sense that it allows for any kind of point-mass beliefs about wages and rents, in our analysis below we assume that the expected prices are the equilibrium wages and rents in a model with the same economic primitives (L, $\{A_n\}$, $\{T_k\}$, $\{\delta_{kn}\}$, α, ϵ, σ) and a continuum of individuals ($I \to \infty$).

3.2 Equilibrium

For expositional clarity, we distinguish between a *trade equilibrium*, which clears markets taking individuals' locations as given, and a *granular commuting equilibrium*, in which a finite number of individuals choose their locations based on beliefs about the trade equilibrium that will result.

Goods market clearing equates each location's output to the quantity demanded. If ℓ_{kn}/δ_{kn} denotes the labor supply of individuals living in k and working in n, then output in location n is $A_n \sum_k \ell_{kn}/\delta_{kn}$. Each individual devotes $1-\alpha$ of their expenditure to differentiated goods and α

[22] With I individuals and N^2 residence-workplace pairs, the set of possible allocations (the support of the multinomial distribution) contains $\binom{I+N^2-1}{N^2-1} = \frac{(I+N^2-1)!}{(N^2-1)!I!}$ elements. For $I = 10$ and $N = 4$, this is about 3.27×10^6.

of their expenditure to land, while immobile landlords spend all of their income on differentiated goods, such that total expenditure on differentiated goods equals aggregate income. The demand for each differentiated good stemming from CES preferences means that equating quantity supplied and quantity demanded requires

$$A_n \sum_k \frac{\ell_{kn}}{\delta_{kn}} = \frac{(w_n/A_n)^{-\sigma}}{P^{1-\sigma}} \sum_{k',n'} \frac{\ell_{k'n'}}{\delta_{k'n'}} w_{n'} \qquad \forall n. \tag{3}$$

Note that goods market clearing implies labor market clearing.

Similarly, land market clearing equates the fixed land endowment T_k to the quantity demanded by individuals, who devote a constant fraction α of their expenditure to land:

$$T_k = \frac{\alpha}{r_k} \sum_n \frac{\ell_{kn}}{\delta_{kn}} w_n \qquad \forall k. \tag{4}$$

We next define the *trade equilibrium*, which clears markets taking individuals' locations as given.

Definition 3.1. Trade equilibrium. Given the labor allocation $\{\ell_{kn}\}$ and economic primitives (L, $\{A_n\}$, $\{T_k\}$, $\{\delta_{kn}\}$, α, ϵ, σ), a trade equilibrium is a set of wages $\{w_n\}$ and land prices $\{r_k\}$ such that equations (3) and (4) are satisfied.

Remark. Given the labor allocation $\{\ell_{kn}\}$, there is a unique set of wages and land prices satisfying equations (3) and (4). Since $\sigma > 1$, there is a unique set of wages satisfying equation (3), by application of Theorem 1 of Allen, Arkolakis, and Takahashi (2020). Equation (4) can be rewritten as $r_k = \frac{\alpha}{T_k} \sum_n \frac{\ell_{kn}}{\delta_{kn}} w_n$, so there is a unique set of land prices associated with that wage vector.

Individuals' choices of location are made on the basis of their beliefs about the subsequent trade equilibrium. Given belief vectors $\{\tilde{w}_n\}$ and $\{\tilde{r}_k\}$ and the distribution of $\{\nu^i_{kn}\}$, equation (2) implies that the probability of any individual choosing kn as her residence-workplace pair is

$$\Pr(U^i_{kn} > U^i_{k'n'} \ \forall (k',n') \neq (k,n)) = \frac{\tilde{w}_n^{\epsilon} \left(\tilde{r}_k^{\alpha} \delta_{kn}\right)^{-\epsilon}}{\sum_{k',n'} \tilde{w}_{n'}^{\epsilon} \left(\tilde{r}_{k'}^{\alpha} \delta_{k'n'}\right)^{-\epsilon}}. \tag{5}$$

With these probabilities in hand, we define a granular commuting equilibrium as the labor allocation resulting from drawing I realizations of this process and clearing markets.

Definition 3.2. Granular commuting equilibrium. Given a number of individuals I, economic primitives (L, $\{A_n\}$, $\{T_k\}$, $\{\delta_{kn}\}$, α, ϵ, σ), and a set of point-mass beliefs ($\{\tilde{w}_n\}, \{\tilde{r}_k\}$), a granular commuting equilibrium is a labor allocation $\{\ell_{kn}\}$, wages $\{w_n\}$, and land prices $\{r_k\}$ such that

- $\ell_{kn} = \frac{L}{I} \sum_{i=1}^{I} \mathbf{1}\{\tilde{U}^i_{kn} > \tilde{U}^i_{k'n'} \ \forall (k',n') \neq (k,n)\}$ is the labor allocation resulting from I independent draws from the probability mass function in equation (5); and
- wages $\{w_n\}$ and land prices $\{r_k\}$ are a trade equilibrium, per Definition 3.1, given the labor allocation $\{\ell_{kn}\}$.

Distinguishing between the number of individuals I and the aggregate labor supply L allows us to apply the law of large numbers to locational decisions without changing aggregate labor supply. As Appendix B.1 shows, since I is the number of draws from the probability mass function in equation (5), fixing L and taking $I \to \infty$ causes the labor allocation in the limiting case to be

$$\ell_{kn} = L \times \Pr(U^i_{kn} > U^i_{k'n'} \ \forall (k', n') \neq (k, n)) = L \times \frac{\tilde{w}_n^{\epsilon} \left(\tilde{r}_k^{\alpha} \delta_{kn}\right)^{-\epsilon}}{\sum_{k',n'} \tilde{w}_{n'}^{\epsilon} \left(\tilde{r}_{k'}^{\alpha} \delta_{k'n'}\right)^{-\epsilon}}. \tag{6}$$

Note that this limiting labor allocation still depends on beliefs. We now define the idea that, for this limiting case, rational expectations are point-mass beliefs that coincide with the resulting wages and prices.

Definition 3.3. Rational expectations for the continuum case. Given economic primitives (L, $\{A_n\}$, $\{T_k\}$, $\{\delta_{kn}\}$, α, ϵ, σ), $\{\tilde{w}_n\}$ and $\{\tilde{r}_k\}$ are "continuum-case rational expectations" if $\{\tilde{w}_n\}$ and $\{\tilde{r}_k\}$ constitute a trade equilibrium for the labor allocation $\{\ell_{kn}\}$ given in equation (6).

As $I \to \infty$, if individuals' point-mass beliefs are continuum-case rational expectations, then the model coincides with the standard continuum model of Redding and Rossi-Hansberg (2017). That is, combining equations (3) and (4) with equation (6) evaluated at $\tilde{w}_n = w_n$ and $\tilde{r}_k = r_k$ is the standard spatial-equilibrium model with a continuum of individuals.[23]

For finite I, a given set of economic primitives (L, $\{A_n\}$, $\{T_k\}$, $\{\delta_{kn}\}$, α, ϵ, σ) and point-mass beliefs ($\{\tilde{w}_n, \tilde{r}_k\}$) generate a *distribution* of equilibria associated with realizations of the process generating ν^i_{kn} and hence $\{\ell_{kn}\}$.[24]

Even though our implementation of the granular model uses the continuum model to generate expectations for wages and rents, our granular framework differs from the conventional model in fundamental ways. First, the granular model can generate zeros as outcomes for residence-workplace pairs without assuming infinite commuting costs. Second, the granular model can rationalize the observed positive commuting flows when commuting costs are a parsimonious function of transit times, such as $\delta_{kn} = f(\text{transit time}_{kn})$. By contrast, the continuum model cannot rationalize the data with such a specification, so it requires many more (and different) structural parameters, which can lead to overfitting.

4 Estimation

In this section, we apply the model to the tract-to-tract commuting data from Detroit and New York City discussed in Section 2. Section 4.1 describes the estimation procedure. Section 4.2

[23] In the absence of agglomeration forces, this quantitative spatial model with a continuum of individuals has a unique equilibrium (see Ahlfeldt et al. (2015)). Therefore, the continuum-case rational expectations of wages and land rents are unique.

[24] Redding and Rossi-Hansberg (2017, p.38) anticipated this implication of granularity: "At smaller spatial scales (e.g., blocks within cities), one might expect such random idiosyncratic factors to be more important relative to the systematic deterministic components of a model (e.g., natural resource abundance) than at larger spatial scales (e.g., across regions or countries)."

reports the estimation results and contrasts them with estimates from other methods.

4.1 Estimation procedure

We assume each individual supplies one unit of labor, so that $L = I$ is equal to the number of employed individuals. We follow the literature to obtain values of α and σ. We impose $\alpha = 0.24$, based on Davis and Ortalo-Magne (2011), and $\sigma = 4$, following Monte, Redding, and Rossi-Hansberg (2018).

We estimate the remaining model parameters ($\{\delta_{kn}\}$, ϵ, $\{\tilde{r}_k\}$, $\{\tilde{w}_n\}$, $\{T_k\}$, $\{A_n\}$) by the following three steps:

1. we compute commuting costs $\{\delta_{kn}\}$ using transit times;
2. we estimate the commuting elasticity, ϵ, and the beliefs about wages and rents, $\{\tilde{r}_k\}$, $\{\tilde{w}_n\}$, using data on commuting counts $\{\ell_{kn}\}$; and
3. we infer location fundamentals ($\{T_k\}, \{A_n\}$) by assuming that the wage and rent beliefs are continuum-case rational expectations.

4.1.1 Commuting costs

We compute commuting costs by assuming that each worker has an exogenous endowment of H hours that is spent either working or commuting. In the baseline parameterization, we assume $H = 9$.[25] We then construct the commuting costs as $\delta_{kn} = \frac{H}{H - t_{kn} - t_{nk}}$, where t_{kn} is the transit time from k to n according to Google Maps.[26] Given H hours, $1/\delta_{kn}$ is the share of that time spent working if the individual resides in k and works in n.

4.1.2 Estimation of commuting elasticity and wage and rent beliefs

Given observable values of commuting costs δ_{kn}, the commuting elasticity ϵ can be estimated by maximum likelihood. Using the probability mass function in equation (5) and denoting the number of individuals who chose the kn pair by ℓ_{kn}, the log likelihood function is

$$\ln \mathcal{L} \equiv \sum_k \sum_n \ell_{kn} \ln \left[\Pr(U^i_{kn} > U^i_{k'n'} \ \forall (k', n') \neq (k, n)) \right] = \sum_k \sum_n \ell_{kn} \ln \left[\frac{\tilde{w}_n^{\epsilon} \left(\tilde{r}_k^{\alpha} \delta_{kn} \right)^{-\epsilon}}{\sum_{k', n'} \tilde{w}_{n'}^{\epsilon} \left(\tilde{r}_{k'}^{\alpha} \delta_{k'n'} \right)^{-\epsilon}} \right].$$

As shown by Guimarães, Figueirdo, and Woodward (2003), the maximization of this likelihood function is numerically equivalent to a Poisson pseudo-maximum-likelihood estimator that is avail-

[25] Using $H = 8$ or $H = 10$ yields very little change in model fit relative to the $H = 9$ results reported in Table 4.

[26] For Detroit, we use Google Maps driving times collected by Owens, Rossi-Hansberg, and Sarte (2020). For New York City, we use Google Maps public-transit times collected by Davis et al. (2019). We impute missing observations by predicting transit times using physical distance, imputing transit times for fewer than 0.3% of tract pairs in Detroit and fewer than 4.1% of tract pairs in New York City.

able for a variety of software packages.[27]

Individuals' beliefs about wages and land prices can be inferred from the same maximum likelihood estimates. Given values of the commuting elasticity ϵ and the land expenditure share α, the beliefs $\{\tilde{r}_k\}$ and $\{\tilde{w}_n\}$ can be recovered from transformations of the gravity equation's origin fixed effects and destination fixed effects. In particular, in equation (5) the origin fixed effect is proportionate to $\tilde{r}_k^{-\alpha\epsilon}$ and the destination fixed effect is proportionate to $\tilde{w}_n^{\epsilon}$.

4.1.3 Estimation of location fundamentals

The economic primitives $\{T_k\}$ and $\{A_n\}$ can be inferred by assuming that individuals' beliefs are continuum-case rational expectations. Using the values of α, ϵ, and $\{\delta_{kn}\}$ described above, plugging our estimates of the beliefs $\{\tilde{r}_k\}$ and $\{\tilde{w}_n\}$ into equation (6) yields the continuum-case labor allocation. Given α, σ, $\{\tilde{r}_k\}$, $\{\tilde{w}_n\}$, $\{\delta_{kn}\}$ and that continuum-case labor allocation, equations (3) and (4) can be solved to yield values of $\{T_k\}$ and $\{A_n\}$.

4.2 Estimation results

We next describe our estimation results. Our baseline commuting cost elasticity estimate is presented in column 1 of Table 4. We estimate only modest dispersion of the idiosyncratic utility draws, leading to estimates of $\epsilon \approx 20$ for Detroit and $\epsilon \approx 8$ for New York City.

These elasticity estimates are substantially altered if we apply procedures used in the prior literature to handle observations with zero commuters. While the granular model's likelihood function accommodates zero commuters for some pairs of locations, most prior work has estimated the commuting gravity equation based on a log-linear transformation of equation (6) after dropping all observations with zero commuters.[28] Columns 2 and 3 illustrate that dropping the tract pairs with zero flows leads to substantially smaller estimates of ϵ, about one-half to two-thirds the magnitude of the estimates in column 1.[29] A less common practice is to recode zero-value observations to small numbers before estimating via OLS.[30] Column 4 illustrates that recoding zeros to small positive numbers yields estimates of the elasticity (and accompanying standard errors) that are an order of magnitude larger in absolute value. These differences in estimated elasticities are due to differences in the handling of zeros, not our use of transit times to measure commuting costs, as shown in Appendix C.

Some prior work (e.g., Krebs and Pflüger 2019) has applied the Poisson PML estimator to

[27] See Sotelo (2019) for a discussion of the relationship between the multinomial and Poisson pseudo-maximum-likelihood estimators in the context of gravity models. In practice, we use the Stata package `ppmlhdfe` of Correia, Guimarães, and Zylkin (2019).

[28] Among others, Heblich, Redding, and Sturm (2018); Monte, Redding, and Rossi-Hansberg (2018); Severen (2019); Tsivanidis (2019) drop pairs of geographic units with zero commuters.

[29] The selection bias is most clearly illustrated by contrasting columns 1 and 2. Columns 1 and 3 differ both in estimation sample and estimator.

[30] In spatial economics, Owens, Rossi-Hansberg, and Sarte (2020) replace $\ell_{kn} = 0$ by $10^{-12} \times \ell_{nn}$. See Gandhi, Lu, and Shi (2019) and Dubé, Hortaçsu, and Joo (2020) for discussions of such ad hoc approaches to handling zero-value market shares in the context of discrete-choice demand estimation.

Table 4: Commuting elasticity estimates

	(1) MLE	(2) MLE non-zero	(3) OLS non-zero	(4) OLS recode
Panel A. Detroit (2014)				
Commuting cost	-19.81	-14.08	-8.958	-85.41
	(0.307)	(0.227)	(0.168)	(1.606)
Model fit (R^2 or pseudo-R^2)	0.619	0.466	0.533	0.365
Location pairs	1,353,726	358,361	358,361	1,246,772
Commuters	1,307,096	1,307,096	1,307,096	1,307,096
Panel B. New York City (2010)				
Commuting cost	-7.986	-4.357	-2.307	-17.95
	(0.307)	(0.201)	(0.0516)	(0.339)
Model fit (R^2 or pseudo-R^2)	0.662	0.504	0.561	0.350
Location pairs	4,628,878	690,673	690,673	4,434,731
Commuters	2,488,905	2,488,905	2,488,905	2,488,905

Standard errors, two-way clustered by k and n, in parentheses

NOTES: All specifications include destination fixed effects and origin fixed effects. Column 1 presents the results from the maximum likelihood estimation described in Section 4.1.2. Column 2 presents the results from applying the maximum likelihood estimator to a sample that omits observations with zero commuters. Column 3 estimates the gravity equation in logs via OLS. Column 4 recodes $\ell_{kn} = 0$ observations to $\ell_{kn} = 10^{-12}\ell_{nn}$ before estimating the gravity equation in logs via OLS. The model-fit statistic is the pseudo-R^2 in columns 1 and 2 and R^2 in columns 3 and 4.

equation (6). Such an approach produces point estimates for the elasticity that are identical to those in column 1. However, in a model with a continuum of individuals, all positive-probability events do occur in equilibrium, so the only way to rationalize zero flows is to assume an infinite commuting cost on that route to make it a zero-probability event. Applying the Poisson PML estimator in line with the continuum model's assumption would involve dropping zero-commuter observations and producing the elasticity estimates in column 2 of Table 4. With a continuum model, the pairing of the estimator and sample used to produce column 1 is theoretically inconsistent.

Using our estimates corresponding to column 1 of Table 4, we recover the locational fundamentals by assuming that the wage and rent beliefs are continuum-case rational expectations. Per equation (5), given α and ϵ, the origin fixed effects and destination fixed effects reveal (relative) wage and rent beliefs. Applying Definition 3.3, these beliefs reveal locations' relative productivities and land endowments.

Dropping observations with zero commuters can substantially alter the estimated origin and destination fixed effects in equation (5). When only using positive-commuter observations, these fixed effects characterize the average number of commuters for a residence-workplace pair, conditional on the number of commuters being strictly greater than zero. For destinations with small numbers of employees, this conditional average is greater than the unconditional average. Figure 3 contrasts

Figure 3: Destination fixed effects from tract-to-tract gravity regressions

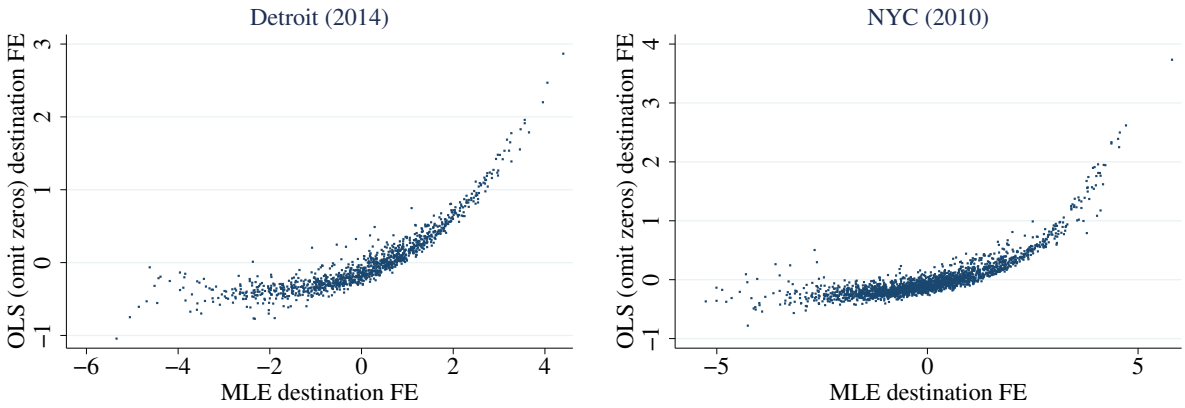

NOTES: These plots depict the destination fixed effects estimated in Table 4's column 1 (horizontal axis) and column 3 (vertical axis). The left panel plots these fixed effects for Detroit; the right panel plots them for New York City. See the notes to Table 4 for details.

the OLS (vertical axis) and maximum likelihood (horizontal axis) estimates of the destination fixed effects. The difference is stark: the range of the OLS estimates is half that of the maximum-likelihood estimates due to considerable truncation from below. In essence, the popular practice of omitting zero-commuter observations attributes low-employment destinations' lower employment counts to infinite commuting costs, not lower wage beliefs (lower productivity).[31] By contrast, our maximum likelihood estimator infers that these destinations are unattractive workplaces from the fact that many origins have zero residents working in these destinations.

5 Counterfactual analysis and event studies

Researchers employing quantitative spatial models aim to provide a parsimonious general-equilibrium framework in order to predict counterfactual outcomes.[32] The value of these quantitative models for policy analysis therefore depends largely on their ability to predict the spatial distribution of economic consequences of a shock.[33] Oftentimes, quantitative spatial models are calibrated to exactly replicate the observed spatial distribution of economic outcomes before introducing

[31] Census tracts are defined so that the number of residents is similar across tracts, while there is tremendous heterogeneity in total employment. Thus, the selection bias is evident in the destination fixed effects. When estimating the analogous gravity regression for county-to-county commuting flows, we find that the selection bias manifests in both the origin and destination fixed effects. See Appendix C.

[32] Redding and Rossi-Hansberg (2017, p.23): "[T]his research does not aim to provide a fundamental explanation for the agglomeration of economic activity, but rather to provide an empirically relevant quantitative model to perform general equilibrium counterfactual policy exercises." Waddell and Sarte (2016, p.190): "The development of the new quantitative equilibrium models has initiated a more robust and realistic framework with which to model cities... By offering a more accurate grounding for empirical models, it will also allow for more robust counterfactual policy exercises that can inform practitioners and policymakers regarding strategies for urban development."

[33] Bryan, Glaeser, and Tsivanidis (2019, p.31): "If quantitative models are to provide useful policy insights, their results have to be trusted. First, researchers must establish that their model captures relevant features of the data or (ideally) can replicate the real-world response to a policy change."

counterfactual changes in parameters.[34] In granular settings, this calibrated-shares procedure suffers the defect of overfitting outcomes that reflect individuals' idiosyncratic choices rather than persistent economic features. Such overfitting could reduce its predictive power.

The following sections contrast counterfactual analysis in our granular framework with the calibrated-shares procedure. Section 5.1 describes and contrasts the two approaches to analyzing outcomes in counterfactual scenarios. Section 5.2 contrasts the nature of the predicted incidence of local productivity shocks using the example of Detroit. Section 5.3 examines each approach's ability to predict changes in commuting patterns associated with tract-level employment booms in New York City. We find that the granular model outperforms the conventional calibrated-shares procedure in the vast majority of events.[35] Section 5.4 examines the potential for pooling observations across years to improve predictive power and finds that the granular model still outperforms the calibrated-shares procedure.

5.1 Counterfactual analysis in spatial models

Our granular framework yields counterfactual predictions that differ from those of models with a continuum of individuals for two reasons: different estimated parameter values and different counterfactual outcomes given parameter values. The estimated parameter values differ because the continuum approach equates model probabilities and observed outcomes, whereas our granular framework's maximum-likelihood estimator allows these to differ. Given common parameter values, the continuum approach typically predicts a unique counterfactual equilibrium (a deterministic distribution), whereas our granular framework yields a distribution of equilibrium outcomes associated with the granular data-generating process due to the distribution of idiosyncratic preference shocks.

Calibrating quantitative spatial models to exactly replicate the observed spatial distribution of economic outcomes equates model probabilities and observed shares. This has substantial consequences for inferred amenities, productivities, and commuting costs. Most notably, this procedure infers that unchosen outcomes are zero-probability events, thereby assigning infinite commuting costs to residence-workplace pairs with zero commuters.[36] More broadly, equating relative probabilities with relative counts means that structural parameters are often inferred from "lumpy" comparisons of one versus two versus three commuters.

While not all the parameters of quantitative spatial models are identified by this calibrated-shares procedure, it allows one to compute the counterfactual equilibrium outcomes associated with a proportionate changes in these parameters.[37] In Appendix D, we apply this calibrated-

[34] Waddell and Sarte (2016, p.188): "[C]ounterfactual exercises involving a change to some exogenous aspect of the city, or a change in urban policy, are rooted in a model that, as a benchmark, is able to exactly match basic observed allocations and prices in the city as equilibrium outcomes." This calibration approach has roots in the quantitative trade practice called "calibrated share form" or "exact hat algebra" (Rutherford, 1995; Dekle, Eaton, and Kortum, 2008).

[35] Kehoe (2003) argues that "it is the responsibility of modelers to demonstrate that their models are capable of predicting observed changes, at least ex post."

[36] For example, see Monte, Redding, and Rossi-Hansberg (2018, p.3869); Heblich, Redding, and Sturm (2018, p.22); and Severen (2019, p.7).

[37] For example, see Monte, Redding, and Rossi-Hansberg (2018, p.3866-7); Krebs and Pflüger (2019, p.32); and

shares procedure to the continuum-of-individuals variant of the model in Section 3. Given a labor allocation $\{\ell_{kn}\}$, wages $\{w_n\}$, labor demand elasticity σ, and commuting elasticity ϵ, one can compute proportionate changes in wages, rents, and labor allocations for any combination of proportionate changes in productivity $\{\hat{A}_n\}$, land $\{\hat{T}_k\}$, and commuting costs $\{\hat{\delta}_{kn}\}$. Implicitly, the procedure calibrates initial combinations $\{A_n\}$, $\{T_k\}$, and $\{\delta_{kn}\}$ that rationalize the (observed) initial equilibrium values of $\{\ell_{kn}\}$ and wages $\{w_n\}$.

By contrast, we estimate the parameters of our granular model without perfectly equating model probabilities and observed outcomes. Our maximum-likelihood estimator assumes that the commuting cost δ_{kn} is a function of observed covariates, so that the number of underlying commuting-cost parameters is smaller than the number of commuting observations. While the parsimonious specification employed in Section 4 assumes that δ_{kn} is solely a function of Google Maps transit times, one could employ far more flexible forms (such as interactive fixed effects or regularization of pair fixed effects) without exhausting the available degrees of freedom. Since model probabilities and equilibrium outcomes are not identical in our approach, there is a distribution of counterfactual equilibrium outcomes associated with counterfactual parameter values. In particular, different values of the idiosyncratic preference shocks $\{\nu^i_{kn}\}$ generate different equilibrium allocations and prices for the same counterfactual values of economic primitives. In practice, we numerically simulate the model many times and present moments that summarize this distribution of counterfactual outcomes.

5.2 Contrasting predictions for the incidence of shocks

As a first means of contrasting the calibrated-shares procedure with our granular approach, we examine the predicted changes in land prices induced by a productivity increase in one workplace location. We apply each procedure to the Detroit urban area, using census tracts as the spatial units of interest and 2014 values as the initial equilibrium. The counterfactual change is a 20% increase in the productivity level of one census tract that has total employment at the 70^{th} percentile of the workplace employment distribution.

Figure 4 depicts the (mean) predicted changes in land prices produced by each procedure and the initial distribution of residents who in 2014 worked in the "treated" tract that has higher productivity in the counterfactual scenario. The calibrated-shares procedure's predictions for changes in land prices depicted in the upper-left panel are highly correlated (0.88) with the initial distribution of residents depicted in the bottom panel. Intuitively, the spatial incidence of a productivity increase across different locations' residential land prices is due to an increase in the workplace wage making residential locations that have low costs of commuting to that workplace more likely to be chosen. Since the majority of census tracts were home to zero residents who worked in the treated tract in 2014, the calibrated-shares procedure says that the cost of commuting from these residential locations to the treated workplace is infinity. As a result, these residential locations are almost entirely unaffected by the counterfactual change in that tract's productivity.

Severen (2019, p.30).

Figure 4: Calibrated-shares procedure's predicted changes in land prices closely follow initial shares

(a) Calibrated-shares land-price changes

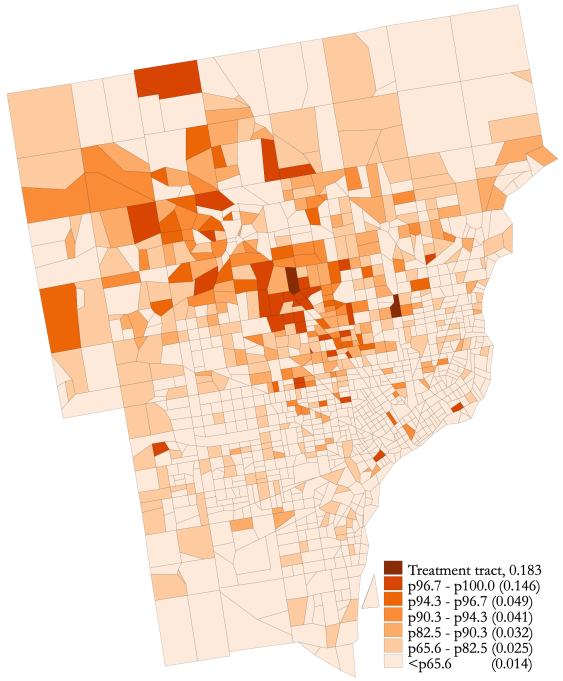

(b) Granular model's mean land-price changes

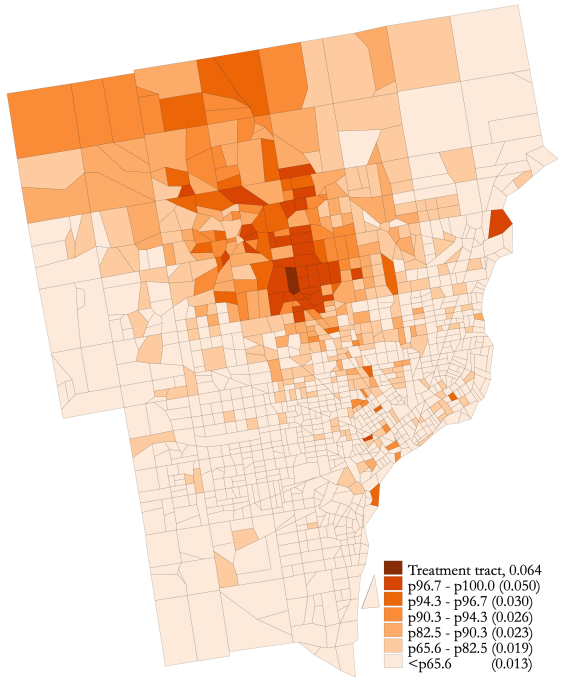

(c) Number of residents in baseline data

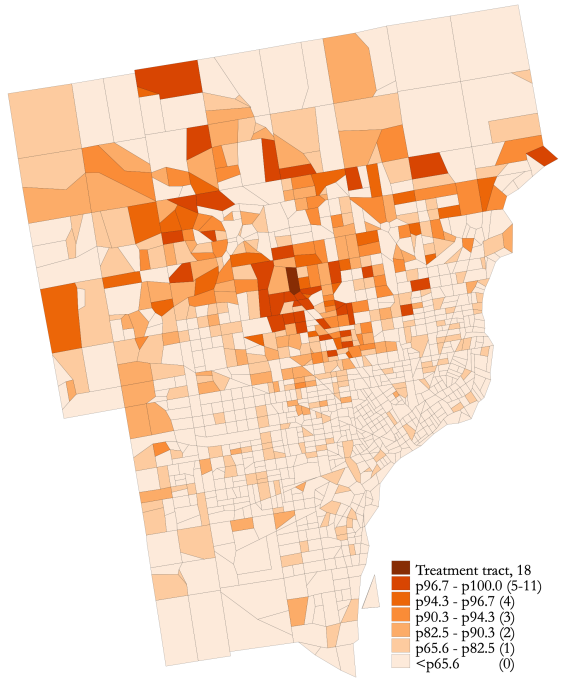

NOTES: These maps depict the tracts of the Detroit urban area. We consider the incidence of a 20% productivity increase in the treated tract, which has total employment at the 70^{th} percentile of the workplace employment distribution. The map in the upper-left panel depicts each tract's percentage-point change in the price of land (r_k/P) computed using the calibrated-shares procedure. The map in the upper-right panel depicts each tract's percentage-point change in the mean counterfactual land price from the mean baseline land price across one million simulations of the granular model for both the baseline and counterfactual parameter values. The map in the lower panel depicts the number of residents in each tract who work in the treated tract in the observed data that is perfectly rationalized by the calibrated-shares procedure. In the legend, the number within parentheses denotes the value of the percentile that is the upper bound of each percentile range.

By contrast, in our granular framework the bilateral commuting cost is a function of transit time, so locations that had zero residents working in the treated tract in 2014 may have residents who work in that workplace in counterfactual equilibria. Thus, the increase in productivity triggers increases in land prices in neighboring locations that have short commutes to the treated tract. The upper-right panel of Figure 4 depicts the percentage-point change in the mean counterfactual land price from the mean baseline land price for each tract across one million simulations of the granular model for both the baseline and counterfactual parameter values. The mean incidence of the productivity change on land prices is mildly correlated (0.40) with the initial distribution of residents and more clearly connected to physical proximity to the treated tract.

Next, we use the estimated model to assess the sensitivity of equilibrium land prices to the idiosyncratic component of individuals' choices. We quantify the role of granularity by examining how much equilibrium land prices vary across different equilibria generated by the same fundamental parameters. The mean land prices across one million simulations are centered on the continuum-case rational expectation values: across 1,166 tracts, the largest difference is less than 0.05%. Variation in land-price changes around the mean changes depicted in Figure 4 reveals how far this empirical setting is from the limiting case. Figure 5 summarizes land-price variation across one million simulations of the impact of the productivity increase in the treated tract. It is clear that the mean changes in land prices associated with the productivity increase are quite small relative to the granular "noise." The 5^{th} percentile land-price change is less than zero and the 95^{th} percentile is greater than zero for all locations. The magnitude of the mean predicted incidence of this productivity change on local land prices pales in comparison to the idiosyncratic component of equilibrium outcomes that is attributable to granularity. Thus, while economists may be able to compute numerous counterfactual outcomes for small spatial units, they should also quantify their forecasts' precision and sensitivity to granularity.

5.3 Event studies: Predicting observed commuting responses to a local shock

We now examine each approach's predicted commuting patterns for a large, discrete change in employment in a single census tract. Quantitative spatial models typically rationalize increases in local labor demand as increases in local productivity. For each event, we use both our estimated granular model and the popular calibrated-shares procedure to predict the changes in the number of commuters from each residential location to the "treated" workplace tract in which employment increased. These are the spatial linkages that govern quantitative spatial models' predictions about the incidence of local economic shocks on outcomes like land prices. The arrival of a new tenant that substantially boosted tract-level employment constitutes a large local economic shock accompanied by substantial changes in commuting counts. Examining these outcomes assesses these models' characterization of spatial linkages without requiring that the increase in total employment in the destination tract be exogenous to local economic outcomes.[38] Of course, a number of concurrent

[38] As shown in the previous section, spatial linkages are critical to quantitative spatial models' predictions about incidence of a productivity increase. Studying changes in commuter counts addresses the limited data on tract-level

Figure 5: Distribution of changes in land prices

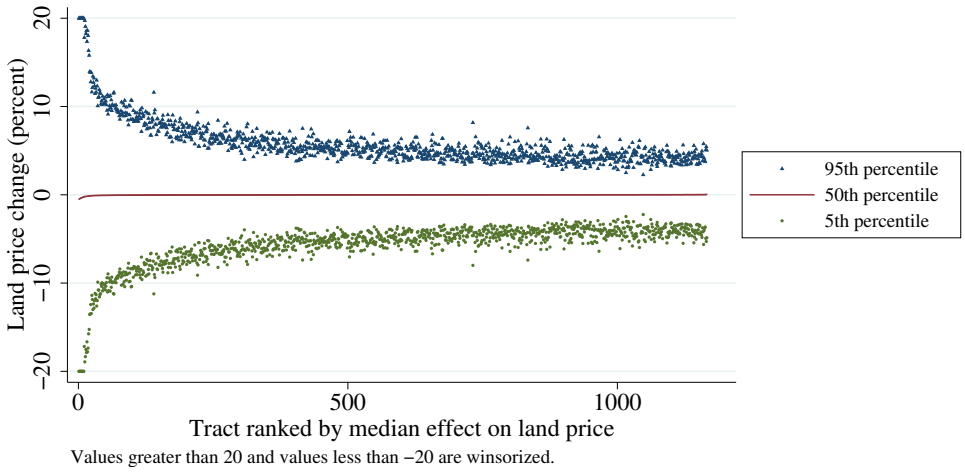

NOTES: This figure summarizes variation in land prices (r_k/P) across 1,000,000 simulations of the impact of the productivity increase described in the notes of Figure 4. For each tract, it depicts the 5^{th}, 50^{th}, and 95^{th} percentile of the land-price change distribution for 1,000,000 simulations at the new parameter values relative to the mean land price for 1,000,000 simulations at the old parameter values.

changes in the city will cause the observed changes to differ from the predictions of these models generated by increasing productivity in this workplace to increase total employment while leaving all other parameters at their values estimated using the initial observed outcomes. Comparing relative predictive power is informative about the relative value of these economic models for counterfactual analysis.

To begin, we study two events in New York City in which the arrival of a large employer increased local employment.[39] The first event we study is the 2010–2012 change in employment in the census tract in New York City that contains 200 Fifth Avenue. This building in the Flatiron District was converted from a toy showroom into Class A office space by a developer over 2007–2009. In 2011, Tiffany & Co. moved into 260,000 square feet of office space at 200 Fifth Avenue, uniting employees who previously had been spread across three different offices. Our second event study focuses on the tract containing 111 Eighth Avenue, a building of nearly 3 million square feet that Google acquired in late 2010. The time series for total employment in each of the tracts studied are depicted in Figure D.1.

We estimate or calibrate the model based on 2010 data for New York City. We estimate our granular model using data on tract-to-tract commuting flows by maximum likelihood, as described in Section 4. The calibrated-shares procedure perfectly rationalizes observed commuting flows and wages, as described in Appendix D.[40] Next, we compute the increase in productivity required

land prices and does not require that the local productivity increase be independent of other local changes that might affect wages and land prices.

[39] We found these events by searching Google News for stories about moves to new offices in New York City.

[40] The largest commuting flow in the 2010 LODES data for New York City is 827 commuters who reside between 110th and 114th Streets in Morningside Heights and work at adjacent Columbia University. The estimated granular

to match the observed 2010-2012 change in employment for the "treated" tract. Since the two procedures fit the 2010 data differently, this productivity increase need not be the same.[41] Since the productivity increases are defined so that both procedures match the observed increase in employment, we examine their predictions for the change in bilateral commuter counts.

Table 5 contrasts the two procedures' predictions for the changes in commuter flows associated with each of the anchor-tenant events. We regress the observed change in the number of residents from each residential tract who work in the treated workplace tract on the predicted change for each procedure. Ideally, a regression of the observed change on the predicted change would yield a slope coefficient of one, an intercept coefficient of zero, and a high R^2. Both procedures fall short of this ideal, as the majority of variation in commuting changes is unexplained by both the granular model (column 1) and the calibrated-shares procedure (column 2). Contrasting the two procedures, the granular model's predictions have lower mean absolute errors and root mean square errors than those of the calibrated-shares procedure for both the Tiffany and Google events.

The granular model's superior predictive power is not due solely to the presence of zeros in the commuting matrix. To illustrate this, we compare the calibrated-shares procedure's predictions to those of a granular model in which commuting costs are infinite for residence-workplace pairs that have zero commuters in the baseline 2010 data. For computational convenience, we use the $I \to \infty$ limit of our granular model, which column 3 of Table 5 shows is very similar to the mean of 1,000 simulations of the granular model. The infinite-commuting-costs variant of the granular model reported in column 4 of Table 5 produces predictions that have lower mean absolute errors and root mean square errors than the predictions of the calibrated-shares procedure. Since the procedures in columns 2 and 4 handle zero-commuter flows identically, the granular model's superior predictive performance is due in part to better predicting commuter-count changes for residence-workplace pairs that have positive counts in the baseline 2010 data.

Next, we scale up our inquiry by examining numerous workplace tracts that experienced substantial employment growth from 2010 to 2012. We conduct an "event study" for each of the 78 workplace tracts in New York City that had a two-year increase in total employment of at least 500 employees and at least 15% from a 2010 level of at least 500 employees. Though the narrative behind each of these employment booms is not as clear as the two anchor-tenant events described above, this greatly expanded scope of inquiry allows us to generalize the contrast between the predictive performance of our granular model and the calibrated-shares procedure.

Figure 6 contrasts the two procedures' predictions for the changes in commuter flows associated with all 78 employment booms from 2010 to 2012. For each event, we estimate the slope and intercept when regressing the observed change in commuters on the predicted change in commuters.

model that uses transit times predicts only 197 of the 827 observed commuters, failing to capture the effect of the university's dual role as employer and landlord. The advantage of the calibrated-shares procedure is its potential to capture such linkages.

[41] For the granular model, we compute the productivity increase using the limiting $I \to \infty$ case. This slightly reduces the computational burden of searching over potential productivity increases. We have verified that the average of 1,000 or more granular counterfactual simulations is very similar to the limiting case (under the same parameter values).

Table 5: Observed changes in commuter counts and models' predictions

	(1) Granular (mean)	(2) Calibrated shares	(3) Continuum limit of granular	(4) Continuum limit (prohibitive costs)
Panel A. Tiffany & Co. (200 Fifth Ave.)				
Predicted change	1.641	0.415	1.667	1.472
	(0.119)	(0.0736)	(0.119)	(0.114)
Constant	-0.803	0.732	-0.833	-0.590
	(0.184)	(0.146)	(0.184)	(0.179)
Observations	2,160	2,160	2,160	2,160
R-squared	0.081	0.014	0.083	0.072
Mean absolute error	3.463	3.647	3.461	3.492
Root mean square error	5.089	5.312	5.086	5.101
Panel B. Google (111 Eighth Ave.)				
Predicted change	1.806	0.445	1.811	1.056
	(0.0855)	(0.0409)	(0.0855)	(0.0660)
Constant	-1.001	0.690	-1.008	-0.0692
	(0.132)	(0.0980)	(0.132)	(0.116)
Observations	2,160	2,160	2,160	2,160
R-squared	0.171	0.052	0.172	0.106
Mean absolute error	2.395	2.642	2.394	2.533
Root mean square error	3.715	4.056	3.714	3.782

NOTES: This table reports OLS regressions for tract pairs in which the dependent variable is the observed change in the number of commuters from each origin tract to the destination tract. Standard errors in parentheses. The independent variables are the model-predicted change in commuters and a constant. The sample consists of pairs of tracts in New York City in which the destination tract is 36061005800 (panel A) or 36061008300 (panel B). The regressor in each column is the change in the number of commuters for that tract pair predicted by the mean of 1,000 simulations of the granular model (column 1), the calibrated-shares procedure (column 2), the $I \to \infty$ limit of the granular model (column 3), and the $I \to \infty$ limit of the granular model after imposing $\delta_{kn} = \infty$ for all observations in which $\ell_{kn} = 0$ in 2010 (column 4). The predictions are generated by calibrating or estimating each model using initial-year data and increasing productivity in the destination tract so that the model's prediction for total employment replicates the observed increase in total employment.

An unbiased prediction procedure should yield a slope of one and an intercept of zero. The upper panel of Figure 6 depicts the distribution of these coefficients for both procedures. For our granular model, the slope coefficients are roughly centered on one (median of 0.95) and the intercept coefficients are roughly centered on zero (median of 0.02). The calibrated-shares procedure does not perform as well. Across the 78 events, the median slope coefficient is -0.24 and the median intercept coefficient is 0.57. That is, the calibrated-shares procedure's predictions are negatively correlated with observed outcomes in more than half the events. As a result, the granular model typically has a lower forecast error. The lower panel of Figure 6 contrasts the two models' root mean squared errors (RMSE) for each event. The granular model has a lower RMSE than the calibrated-shares procedure in 76 of the 78 events. While the calibrated-shares procedure necessarily has better

Figure 6: Comparison of models' predictive performance across 78 events

(a) Coefficients from regressing observed changes on predicted changes

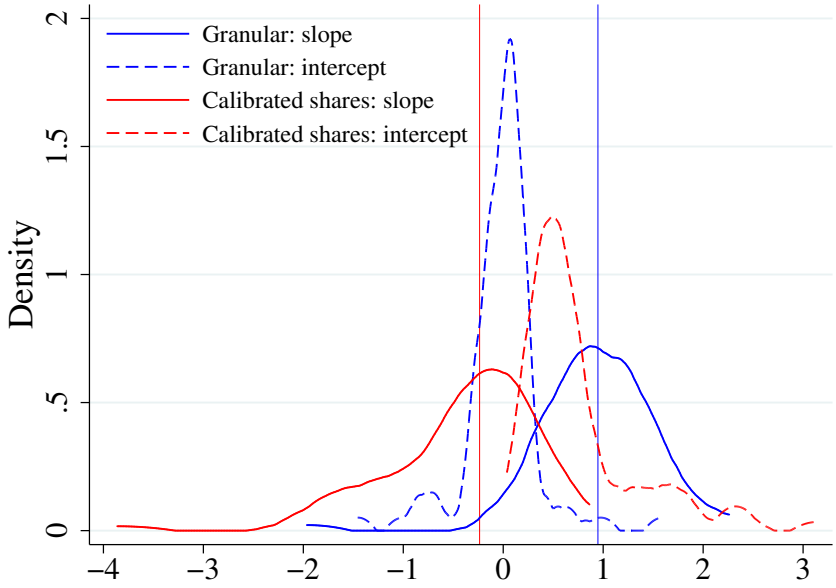

NOTES: 2 outlying calibrated-shares observations not depicted. Vertical lines depict medians of slope coefficient distributions.

(b) Ratio of two models' prediction errors

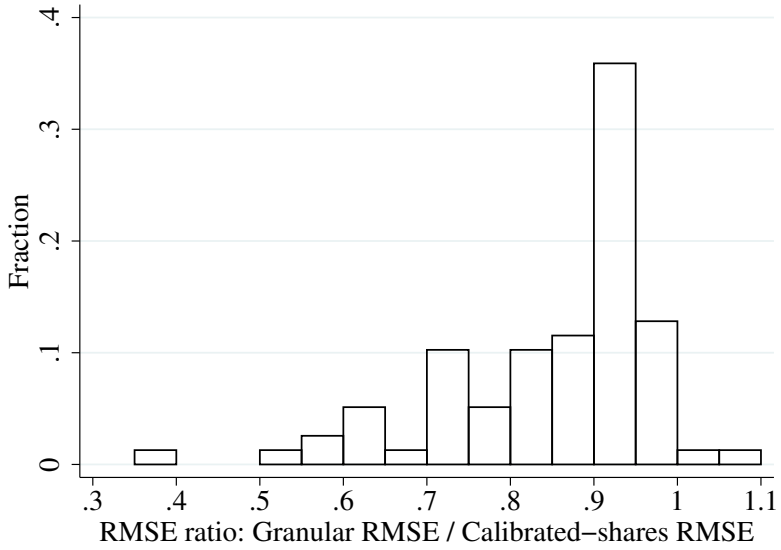

in-sample fit, it falls short when predicting changes in commuting flows.

A Monte Carlo exercise described in detail in Appendix D suggests that this failure could be entirely due to granularity. In the simulations, the data-generating process is our estimated model of New York City in 2010, and we impose a counterfactual productivity increase. With a continuum of individuals, the calibrated-shares procedure would perfectly predict the associated changes in

commuting flows. In practice, the calibrated-shares procedure has very limited predictive power when applied to a finite ($I \approx 2.5$ million) sample drawn from the data-generating process. Thus, granularity alone can severely limit the calibrated-shares procedure's predictive power.

5.4 Alternative prediction strategies

As an alternative to using a granular model, one might consider alternative strategies to "smooth" granular data to be fed into the continuum model. For example, one might hope to eliminate idiosyncratic elements of the data by averaging across multiple years of data.

Averaging multiple years of data could improve the calibrated-shares procedure to the extent that using more years of data is akin to using more observations. In many empirical settings, particularly historical contexts, consecutive years of data are not available. In the case of the LODES data, annual data are available since 2002, and pooling may average out noise introduced by the confidentiality-protecting perturbations mentioned in Section 2.

To explore the gain from pooling multiple years of data, we average commuter and wage observations for 2008-2010 before applying our granular model and the calibrated-shares procedure. As depicted in Figure 7, pooling the data yields a modest improvement for the calibrated-shares procedure. Its predictions are now positively correlated with observed outcomes for more than 60% of the events. Nonetheless, the granular model typically forecasts the changes in commuter counts much better. The granular model's slope coefficients are closer to one (median of 0.95 vs. 0.11) and its intercept coefficients are closer to zero (0.01 vs. 0.38). The granular model applied to the pooled data has a lower RMSE than the pooled calibrated-shares procedure in 65 of the 78 events.

The predictive power of the granular model could potentially be improved further. Recall that our implementation of the granular model uses only transit times to characterize commuting costs, leaving many unused degrees of freedom. Depending on the context, one could add borough-pair fixed effects, interactive fixed effects, or additional covariates such as the frequency of public-transit connections, vehicular transit times, and so forth. By contrast, the calibrated-shares procedure is already a saturated model that uses all degrees of freedom, and therefore its predictive power cannot be easily improved further. Finally, note that the predictive power of the calibrated-shares procedure in these events does not depend on the value of ϵ, since the procedure calibrates the values of $\{\delta_{kn}^{\epsilon}\}$. While the magnitude of the productivity increase $\hat{A}_n$ needed to match the observed employment increase in the destination tract depends on ϵ, the calibrated-shares procedure's predicted commuting-flow changes are invariant to this parameter.

Figure 7: Comparison of models' predictive performance across 78 events (pooled pre-event data)

(a) Coefficients from regressing observed changes on predicted changes

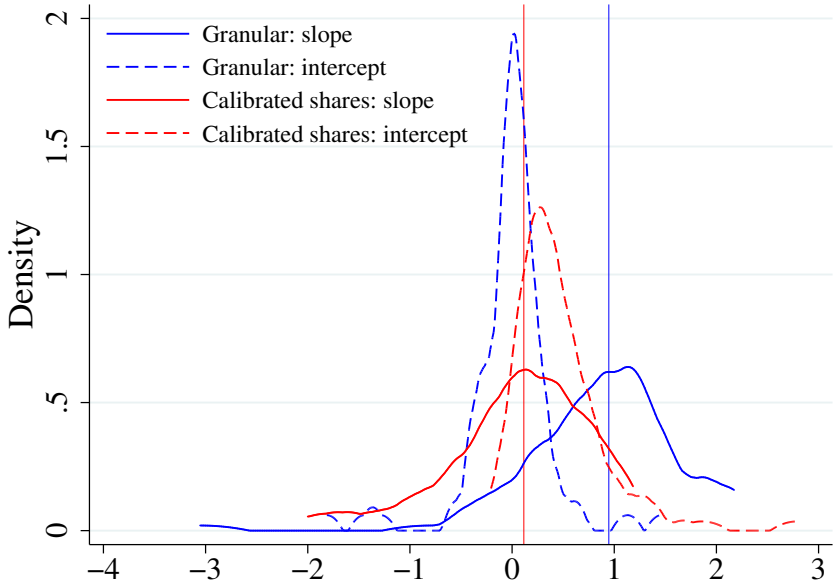

NOTES: 4 outlying calibrated-shares observations not depicted. Vertical lines depict medians of slope coefficient distributions.

(b) Ratio of two models' prediction errors

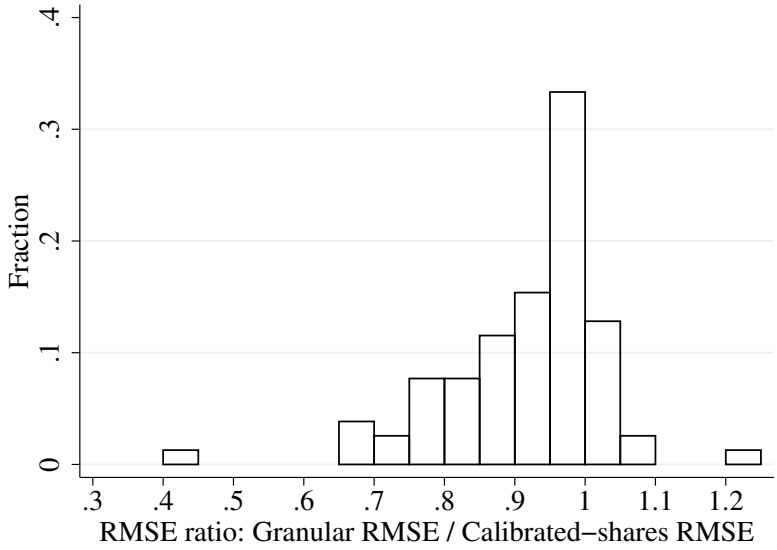

6 Conclusion

Economists increasingly have access to spatially fine data and use quantitative spatial models to compute counterfactual general-equilibrium outcomes. The smaller the number of individuals behind each economic outcome reported in these data, the less compelling the conventional modeling

assumption that there is a continuum of individuals. We document that empirical settings of interest exhibit granular commuting matrices and discuss the consequences of such granularity for economic modeling, estimation, and predicting counterfactual outcomes. In short, the conventional calibrated-shares procedure risks overfitting in-sample observations at the cost of failing to predict out-of-sample outcomes. We need to evaluate the performance of these applied general-equilibrium models in predicting observed changes if policymakers are going to rely on them to inform their decisions (Kehoe, 2003; Bryan, Glaeser, and Tsivanidis, 2019).

In this paper, we propose a granular model that can generate patterns of outcomes like those in the data, show how to estimate its parameters by maximum likelihood, and contrast its predictions about local economic shocks to those of the conventional continuum model. Assuming that commuting costs for millions of residence-workplace pairs are a parsimonious function of observed covariates rather than millions of pair-specific parameters guards against overfitting granular data. Studying 78 tract-level employment booms in New York City during 2010–2012, we find that our granular model predicts changes in commuting flows better than the calibrated-shares procedure.

Since all empirical settings feature a finite number of individuals, the continuum assumption has been made in the interest of modeling convenience, not realism. Our granular model is equally tractable and leverages the same data as the continuum approach, so it can be applied in the same settings in which economists have thus far assumed a continuum. Moreover, since our granular framework coincides with the standard model in the limit, it can be used to quantify the role of granularity in economic outcomes and assess the (un)suitability of the continuum approximation. Since we have provided evidence that a great variety of spatial settings exhibit granularity, this quantitative framework should find widespread application.

References

Adão, Rodrigo, Costas Arkolakis, and Federico Esposito. 2020. "General Equilibrium Indirect Effects in Space: Theory and Measurement."

Ahlfeldt, Gabriel M., Stephen J. Redding, Daniel M. Sturm, and Nikolaus Wolf. 2015. "The Economics of Density: Evidence From the Berlin Wall." *Econometrica*, 83(6): 2127–2189.

Allen, Treb, and Costas Arkolakis. 2014. "Trade and the Topography of the Spatial Economy." *The Quarterly Journal of Economics*, 129(3): 1085–1140.

Allen, Treb, Costas Arkolakis, and Xiangliang Li. 2015. "Optimal City Structure."

Allen, Treb, Costas Arkolakis, and Yuta Takahashi. 2020. "Universal Gravity." *Journal of Political Economy*, 128(2): 393–433.

Armenter, Roc, and Miklós Koren. 2014. "A Balls-and-Bins Model of Trade." *American Economic Review*, 104(7): 2127–51.

Autor, David H., David Dorn, and Gordon H. Hanson. 2013. "The China Syndrome: Local Labor Market Effects of Import Competition in the United States." *American Economic Review*, 103(6): 2121–68.

Berkes, Enrico, and Ruben Gaetani. 2020. "Income Segregation and Rise of the Knowledge Economy."

Bryan, Gharad, Edward Glaeser, and Nick Tsivanidis. 2019. "Cities in the Developing World." National Bureau of Economic Research Working Paper 26390.

Carvalho, Vasco M., and Basile Grassi. 2019. "Large Firm Dynamics and the Business Cycle." *American Economic Review*, 109(4): 1375–1425.

Correia, Sergio, Paulo Guimarães, and Thomas Zylkin. 2019. "ppmlhdfe: Fast Poisson Estimation with High-Dimensional Fixed Effects."

Couture, Victor, and Jessie Handbury. 2019. "Urban Revival in America."

Daruich, Diego, William Easterly, and Ariell Reshef. 2019. "The surprising instability of export specializations." *Journal of Development Economics*, 137: 36 – 65.

Davis, Donald R., Jonathan I. Dingel, Joan Monras, and Eduardo Morales. 2019. "How Segregated Is Urban Consumption?" *Journal of Political Economy*, 127(4): 1684–1738.

Davis, Morris A., and Francois Ortalo-Magne. 2011. "Household Expenditures, Wages, Rents." *Review of Economic Dynamics*, 14(2): 248–261.

Dekle, Robert, Jonathan Eaton, and Samuel Kortum. 2008. "Global Rebalancing with Gravity: Measuring the Burden of Adjustment." *IMF Staff Papers*, 55(3): 511–540.

di Giovanni, Julian, and Andrei A. Levchenko. 2012. "Country Size, International Trade, and Aggregate Fluctuations in Granular Economies." *Journal of Political Economy*, 120(6): 1083–1132.

di Giovanni, Julian, Andrei A. Levchenko, and Isabelle Mejean. 2014. "Firms, Destinations, and Aggregate Fluctuations." *Econometrica*, 82(4): 1303–1340.

Dingel, Jonathan I. 2017. "The Determinants of Quality Specialization." *Review of Economic Studies*, 84(4): 1551–1582.

Dingel, Jonathan I, Antonio Miscio, and Donald R Davis. 2019. "Cities, Lights, and Skills in Developing Economies." National Bureau of Economic Research Working Paper 25678.

Donaldson, Dave. 2015. "The Gains from Market Integration." *Annual Review of Economics*, 7(1): 619–647.

Dubé, Jean-Pierre H, Ali Hortaçsu, and Joonhwi Joo. 2020. "Random-Coefficients Logit Demand Estimation with Zero-Valued Market Shares." National Bureau of Economic Research Working Paper 26795.

Eaton, Jonathan, and Akiko Tamura. 1994. "Bilateralism and Regionalism in Japanese and U.S. Trade and Direct Foreign Investment Patterns." *Journal of the Japanese and International Economies*, 8(4): 478–510.

Eaton, Jonathan, Samuel Kortum, and Sebastian Sotelo. 2013. "International Trade: Linking Micro and Macro." In *Advances in Economics and Econometrics: Tenth World Congress*. Vol. III, , ed. Eddie Dekel Daron Acemoglu, Manuel Arellano. Cambridge University Press.

Gabaix, Xavier. 2011. "The Granular Origins of Aggregate Fluctuations." *Econometrica*, 79(3): 733–772.

Gandhi, Amit, Zhentong Lu, and Xiaoxia Shi. 2019. "Estimating Demand for Differentiated Products with Zeroes in Market Share Data."

Gaubert, Cecile, and Oleg Itskhoki. 2018. "Granular Comparative Advantage." National Bureau of Economic Research Working Paper 24807.

Graham, Matthew R., Mark J. Kutzbach, and Brian McKenzie. 2014. "Design Comparison of LODES and ACS Commuting Data Products." Center for Economic Studies, U.S. Census Bureau Working Papers 14-38.

Greenstone, Michael, Richard Hornbeck, and Enrico Moretti. 2010. "Identifying Agglomeration Spillovers: Evidence from Winners and Losers of Large Plant Openings." *Journal of Political Economy*, 118(3): 536–598.

Guimarães, Paulo, Octávio Figueirdo, and Douglas Woodward. 2003. "A Tractable Approach to the Firm Location Decision Problem." *The Review of Economics and Statistics*, 85(1): 201–204.

Head, Keith, and Thierry Mayer. 2014. "Chapter 3 - Gravity Equations: Workhorse,Toolkit, and Cookbook." In *Handbook of International Economics*. Vol. 4 of *Handbook of International Economics*, , ed. Gita Gopinath, Elhanan Helpman and Kenneth Rogoff, 131 – 195. Elsevier.

Heblich, Stephan, Stephen J Redding, and Daniel M Sturm. 2018. "The Making of the Modern Metropolis: Evidence from London." National Bureau of Economic Research Working Paper 25047.

Helpman, Elhanan, Marc Melitz, and Yona Rubinstein. 2008. "Estimating Trade Flows: Trading Partners and Trading Volumes*." *The Quarterly Journal of Economics*, 123(2): 441–487.

Holmes, Thomas J., and Holger Sieg. 2015. "Structural Estimation in Urban Economics." In *Handbook of Regional and Urban Economics*. Vol. 5 of *Handbook of Regional and Urban Economics*, , ed. Gilles Duranton, J. Vernon Henderson and William C. Strange, 69 – 114. Elsevier.

Kehoe, Timothy J. 2003. "An evaluation of the performance of applied general equilibrium models of the impact of NAFTA." *Staff Report*.

Krebs, Oliver, and Michael P. Pflüger. 2019. "On the Road (Again): Commuting and Local Employment Elasticities in Germany." Institute of Labor Economics (IZA) IZA Discussion Papers 12257.

Kreindler, Gabriel, and Yuhei Miyauchi. 2020. "Measuring Commuting and Economic Activity inside Cities with Cell Phone Records."

Mogstad, Magne, Joseph P Romano, Azeem Shaikh, and Daniel Wilhelm. 2020. "Inference for Ranks with Applications to Mobility across Neighborhoods and Academic Achievement across Countries." National Bureau of Economic Research Working Paper 26883.

Monte, Ferdinando, Stephen J. Redding, and Esteban Rossi-Hansberg. 2018. "Commuting, Migration, and Local Employment Elasticities." *American Economic Review*, 108(12): 3855–90.

Owens, Raymond, III, Esteban Rossi-Hansberg, and Pierre-Daniel Sarte. 2020. "Rethinking Detroit." *American Economic Journal: Economic Policy*, 12(2): 258–305.

Proost, Stef, and Jacques-François Thisse. 2019. "What Can Be Learned from Spatial Economics?" *Journal of Economic Literature*, 57(3): 575–643.

Quan, Thomas W., and Kevin R. Williams. 2018. "Product variety, across-market demand heterogeneity, and the value of online retail." *The RAND Journal of Economics*, 49(4): 877–913.

Redding, Stephen, and Matthew Turner. 2015. "Transportation Costs and the Spatial Organization of Economic Activity." In . Vol. 5, Chapter 20, 1339–1398. Elsevier.

Redding, Stephen J., and Esteban Rossi-Hansberg. 2017. "Quantitative Spatial Economics." *Annual Review of Economics*, 9(1): 21–58.

Rutherford, Thomas F. 1995. "Constant Elasticity of Substitution Functions: Some Hints and Useful Formulae." Notes prepared for GAMS General Equilibrium Workshop held December, 1995 in Boulder Colorado.

Severen, Christopher. 2019. "Commuting, Labor, and Housing Market Effects of Mass Transportation: Welfare and Identification."

Sotelo, Sebastian. 2019. "Practical Aspects of Implementing the Multinomial PML Estimator."

Train, Kenneth. 2009. *Discrete Choice Methods with Simulation.* Cambridge University Press.

Tsivanidis, Nick. 2019. "Evaluating the Impact of Urban Transit Infrastructure: Evidence from Bogota's TransMilenio."

Waddell, Sonya Ravindranath, and Pierre Daniel Sarte. 2016. "From Stylized to Quantitative Spatial Models of Cities." *Economic Quarterly*, 169–196.

Wollmann, Thomas G. 2018. "Trucks without bailouts: Equilibrium product characteristics for commercial vehicles." *American Economic Review*, 108(6): 1364–1406.

Zárate, Román David. 2019. "Factor Allocation, Informality and Transit Improvements: Evidence from Mexico City."

Appendix – For Online Publication

A Additional results for granular empirical settings

Tract-pair-level commuter counts are so impersistent that a gravity model estimated using an observed bilateral characteristic like transit time or distance can sometimes predict future commuter counts better than the observed value. Table A.1 shows that, for tract pairs with fewer than ten commuters reported, a gravity-based estimate predicts the following year's value better than its current value does. The fitted values from a gravity model estimated using 2013 data have a higher R^2 for predicting observed 2014 values than the observed 2013 values in both Detroit and New York City. Using the observed 2013 values yields better predictions only for the tract pairs with the largest 2% of commuter counts.

Table A.1: Gravity-based estimates predict 2014 commuter counts better than 2013 values do

# of commuters	Share	Gravity: time	2013 values	Share	Gravity: distance	2013 values
Panel A: Detroit						
≤ 5	0.960	0.384	0.307	0.955	0.367	0.307
≤ 10	0.983	0.494	0.473	0.978	0.465	0.472
Panel B: NYC						
≤ 5	0.978	0.364	0.306	0.968	0.373	0.306
≤ 10	0.990	0.476	0.475	0.980	0.477	0.473

NOTES: Each row reports results for all tract pairs in Detroit (upper panel) or New York City (lower panel) with fewer than 5 or 10 commuters in the 2013 LODES data. The "share" columns report the share of tract pairs covered by the row. The first and fourth "share" columns differ because some observations have missing transit-time values. The "gravity" columns report the R^2 obtained by regressing the 2014 number of commuters on the number of commuters predicted by a gravity model estimated using 2013 data. The "2013 values" columns report the R^2 obtained by regressing the 2014 number of commuters on the 2013 number of commuters. The "gravity: time" column estimates the gravity equation (5) as described in Section 4. The "gravity: distance" column uses $\ln \delta_{kn} = \ln \text{distance}_{kn}$ rather than commuting costs defined in Section 4.1.

B Theory

We first demonstrate the claim made in the main text that the continuum model is a limiting case of the granular model. The following subsections present extensions of the bare-bones model in Section 3 that introduce trade costs, local increasing returns, and the use of land in production. The model of perfect competition with local increasing returns should be isomorphic to a model of monopolistic competition with free entry, per the logic in Allen and Arkolakis (2014).

B.1 Continuum model as limiting case of the granular model

We derive the result that the granular model coincides with the continuum model as the number of individuals becomes infinite, $I \to \infty$. Note that aggregate labor supply L is fixed, as each individual supplies L/I units of labor. The key step is to show that equation (6) holds as $I \to \infty$. Conditional on the labor allocation $\{\ell_{kn}\}$, granularity plays no role in the trade equilibrium, which will coincide with that of a continuum model.

Definition 3.2 says that labor supplied by residents of k who work in n is

$$\ell_{kn} = \frac{L}{I} \sum_{i=1}^{I} \mathbf{1}\left\{\tilde{U}^i_{kn} > \tilde{U}^i_{k'n'}, \forall (k',n') \neq (k,n)\right\}.$$

Note that $\mathbf{1}\left\{\tilde{U}^i_{kn} > \tilde{U}^i_{k'n'}, \forall (k',n') \neq (k,n)\right\}$ is a binary random variable that is equal to one with probability $\Pr(\tilde{U}^i_{kn} > \tilde{U}^i_{k'n'}, \forall (k',n') \neq (k,n))$. Thus, $\mathbb{E}\left(\mathbf{1}\left\{\tilde{U}^i_{kn} > \tilde{U}^i_{k'n'}, \forall (k',n') \neq (k,n)\right\}\right) = \Pr\left(\tilde{U}^i_{kn} > \tilde{U}^i_{k'n'}, \forall (k',n') \neq (k,n)\right)$. Since the idiosyncratic preference vectors are independent and identically distributed random variables, the law of large numbers implies that, using equation (5),

$$\begin{aligned}\lim_{I\to\infty} \frac{1}{I} \sum_{i=1}^{I} \mathbf{1}\left\{\tilde{U}^i_{kn} > \tilde{U}^i_{k'n'}, \forall (k',n') \neq (k,n)\right\} &= \mathbb{E}\left(\mathbf{1}\left\{\tilde{U}^i_{kn} > \tilde{U}^i_{k'n'}, \forall (k',n') \neq (k,n)\right\}\right) \\ &= \frac{\tilde{w}^{\epsilon}_n (\tilde{r}^{\alpha}_k \delta_{kn})^{-\epsilon}}{\sum_{k',n'} \tilde{w}^{\epsilon}_{n'} (\tilde{r}^{\alpha}_{k'} \delta_{k'n'})^{-\epsilon}}.\end{aligned}$$

As a result, as $I \to \infty$, $\ell_{kn} \to L \times \frac{\tilde{w}^{\epsilon}_n (\tilde{r}^{\alpha}_k \delta_{kn})^{-\epsilon}}{\sum_{k',n'} \tilde{w}^{\epsilon}_{n'} (\tilde{r}^{\alpha}_{k'} \delta_{k'n'})^{-\epsilon}}$.

B.2 Trade costs

Relative to the model in Section 3, we now assume that goods trade is subject to iceberg trade costs: delivering a unit of the location-n variety to location k requires producing $\tau_{nk} \geq 1$ units in n. Individuals consume differentiated goods at their residences, and the price of location n's output for consumers in location k is $\tau_{nk} w_n / A_n$. Thus, the price index in location k is $\Phi_k = r^{\alpha}_k P^{1-\alpha}_k$, where the local CES price index for goods is $P_k = \left[\sum_n (\tau_{nk} w_n / A_n)^{1-\sigma}\right]^{1/(1-\sigma)}$.

In this environment, the equivalent of equation (2) is such that, based on the beliefs $\{\tilde{w}_n\}$ and $\{\tilde{r}_k\}$, each worker chooses the residential location and the work location that maximize expected

utility,

$$\tilde{U}_{kn}^i = \underbrace{\epsilon \ln\left(\frac{\tilde{w}_n}{\tilde{r}_k^{\alpha}\tilde{P}_k^{1-\alpha}\delta_{kn}}\right)}_{\equiv \tilde{U}_{kn}} + \nu_{kn}^i,$$

where $\tilde{P}_k = \left[\sum_n \left(\tau_{nk}\tilde{w}_n/A_n\right)^{1-\sigma}\right]^{1/(1-\sigma)}$.

With trade costs, the goods-market-clearing condition, which is the equivalent of equation (3), equates quantity supplied and quantity demanded:

$$A_n \sum_k \frac{\ell_{kn}}{\delta_{kn}} = \left(w_n/A_n\right)^{-\sigma} \sum_k \left[\left(\frac{\tau_{nk}}{P_k}\right)^{1-\sigma}\left(\sum_{n'} \frac{\ell_{kn'}}{\delta_{kn'}} w_{n'}\right)\right]. \tag{B.1}$$

Equation (4), which clears the land market, is unchanged by the introduction of trade costs.

The definition of a trade equilibrium is akin to Definition 3.1, with equations (B.1) and (4) serving as the relevant market-clearing conditions.

With trade costs, the expression for the probability of choosing residential-workplace pair kn analogous to equation (5) is

$$\Pr(U_{kn}^i > U_{k'n'}^i \ \forall (k',n') \neq (k,n)) = \frac{\tilde{w}_n^{\epsilon}\left(\tilde{r}_k^{\alpha}\tilde{P}_k^{1-\alpha}\delta_{kn}\right)^{-\epsilon}}{\sum_{k',n'} \tilde{w}_{n'}^{\epsilon}\left(\tilde{r}_{k'}^{\alpha}\tilde{P}_{k'}^{1-\alpha}\delta_{k'n'}\right)^{-\epsilon}}. \tag{B.2}$$

The definition of a granular commuting equilibrium is akin to Definition 3.2 with $\{\tau_{kn}\}$ added to the list of economic primitives and expression (B.2) serving as the relevant probability mass function.

B.3 Local increasing returns

Relative to the model in Section 3, we now assume that production exhibits local external economies of scale. In particular, in each location n the linear production technology is $q_n = A_n L_n$, where L_n is the labor supply of workers working in location n and $A_n \equiv \bar{A}_n L_n^{\eta}$. Thus, the CES price index is $P = \left[\sum_n \left(w_n/(\bar{A}_n L_n^{\eta})\right)^{1-\sigma}\right]^{1/(1-\sigma)}$.

Since output in location n is $\bar{A}_n\left(\sum_k \ell_{kn}/\delta_{kn}\right)^{1+\eta}$, equating quantity supplied and quantity demanded requires

$$\bar{A}_n\left(\sum_k \ell_{kn}/\delta_{kn}\right)^{1+\eta} = \frac{{w_n}^{-\sigma}\bar{A}_n^{\sigma}\left(\sum_k \ell_{kn}/\delta_{kn}\right)^{\eta\sigma}}{P^{1-\sigma}} \sum_{k',n'} \frac{\ell_{k'n'}}{\delta_{k'n'}} w_{n'}. \tag{B.3}$$

The remaining results are unchanged after appropriately substituting in equation (B.3). Equation (4), which clears the land market, and expression (5) are unchanged by the introduction of local increasing returns. The definition of a trade equilibrium is akin to Definition 3.1, with equations (B.3) and (4) serving as the relevant market-clearing conditions. The definition of a

granular commuting equilibrium is akin to Definition 3.2 with $\{\bar{A}_n\}$ and η added to the list of economic primitives.

B.4 Firms produce using land

Relative to the model in Section 3, we now assume that firms produce output using labor and land inputs via a Cobb-Douglas production function. Workers produce in location n with a Cobb-Douglas production technology:

$$q_n = A_n \left(\frac{\phi_n T_n}{\beta} \right)^{\beta} \left(\frac{L_n}{1-\beta} \right)^{1-\beta},$$

where L_n is the labor supply of workers working in location n and ϕ_n is the share of land in location n that is used in production. As a result, the unit cost of production in location n is $c_n = \frac{1}{A_n} r_n^{\beta} w_n^{1-\beta}$. Thus, the CES price index is $P = \left[\sum_n c_n^{1-\sigma} \right]^{1/(1-\sigma)}$.

Since output in location n is $A_n (\phi_n T_n)^{\beta} \left(\sum_k \ell_{kn} \right)^{1-\beta}$, equating quantity supplied and quantity demanded requires

$$A_n (\phi_n T_n)^{\beta} \left(\sum_k \ell_{kn} / \delta_{kn} \right)^{1-\beta} = \frac{(c_n)^{-\sigma}}{P^{1-\sigma}} \sum_{n'} \left(r_{n'} \phi_{n'} T_{n'} + w_{n'} \sum_{k'} \ell_{k'n'} / \delta_{k'n'} \right). \tag{B.4}$$

Equating the fixed land supply T_k to the sum of the quantities of land demanded by firms and by residents requires

$$T_k = \alpha \sum_n \frac{\ell_{kn}}{\delta_{kn}} \frac{w_n}{r_k} + \beta^{\frac{1}{1-\beta}} \left(\frac{w_k}{r_k} \right) \sum_{k'} \frac{\ell_{k'k}}{\delta_{k'k}}. \tag{B.5}$$

The definition of a trade equilibrium is akin to Definition 3.1, with equations (B.4) and (B.5) serving as the relevant market-clearing conditions. The definition of a granular commuting equilibrium is akin to Definition 3.2 with the Cobb-Douglas production parameter β added to the list of economic primitives.

C Estimation results

Much of the prior literature has used measures of distance rather than transit time. Table C.1 shows that the consequences of dropping observations with zero commuters or recoding zero-value observations to small positive numbers reported in Section 4.2 are the same if one uses distance rather than transit time as the observable measure of bilateral commuting costs. Dropping the tract pairs with zero flows produces estimates of the commuting elasticity that are substantially smaller. Recoding zeros to small positive numbers yields estimates of the elasticity that are an order of magnitude larger in absolute value. Similarly, Figure C.1 shows that destination fixed effects are biased by dropping observations with zero commuters, just as shown in Figure 3.

The main text reports gravity regressions for tract-to-tract commuting flows. Table C.2 reports

gravity regressions for county-to-county commuting flows that are analogous to the results reported in Table C.1. The contrasts between columns 1 and 2 and between columns 3 and 4 match those found in the tract-to-tract regressions. Figure C.2 depicts the contrasting origin and destination fixed effects estimated when using all the data and when using only positive observations. Origins that have zero residents working in a greater share of destination counties tend to have higher estimated origin fixed effects when zero-valued observations are omitted from the estimation sample. The same upward bias is also evident for the destination fixed effects.

Table C.1: Commuting elasticity estimates using distance

	(1) MLE	(2) MLE non-zero	(3) OLS non-zero	(4) OLS recode
Panel A. Detroit (2014)				
Distance (log)	-1.098	-0.776	-0.599	-6.629
	(0.0135)	(0.0146)	(0.0128)	(0.110)
Model fit (R^2 or pseudo-R^2)	0.609	0.457	0.539	0.370
Location pairs	1,352,565	357,301	357,301	1,245,712
Commuters	1,281,738	1,281,738	1,281,738	1,281,738
Panel B. New York City (2010)				
Distance (log)	-0.998	-0.562	-0.380	-3.718
	(0.0205)	(0.0168)	(0.00820)	(0.0610)
Model fit (R^2 or pseudo-R^2)	0.673	0.523	0.588	0.362
Location pairs	4,626,742	688,626	688,626	4,432,686
Commuters	2,443,053	2,443,053	2,443,053	2,443,053

Standard errors, two-way clustered by k and n, in parentheses

NOTES: All specifications include destination fixed effects and origin fixed effects. The covariate δ_{kn} is now the geodesic distance between tracts k and n. The estimation sample is restricted to $k \neq n$ observations. Column 1 presents the results from the maximum likelihood estimation described in Section 4.1.2. Column 2 presents the results from applying the maximum likelihood estimator to a sample that omits observations with zero commuters. Column 3 estimates the gravity equation in logs via OLS. Column 4 recodes $\ell_{kn} = 0$ observations to $\ell_{kn} = 10^{-12}\ell_{nn}$ before estimating the gravity equation in logs via OLS. The model-fit statistic is the pseudo-R^2 in columns 1 and 2 and R^2 in columns 3 and 4.

Figure C.1: Destination fixed effects from tract-to-tract gravity regressions with distance covariate

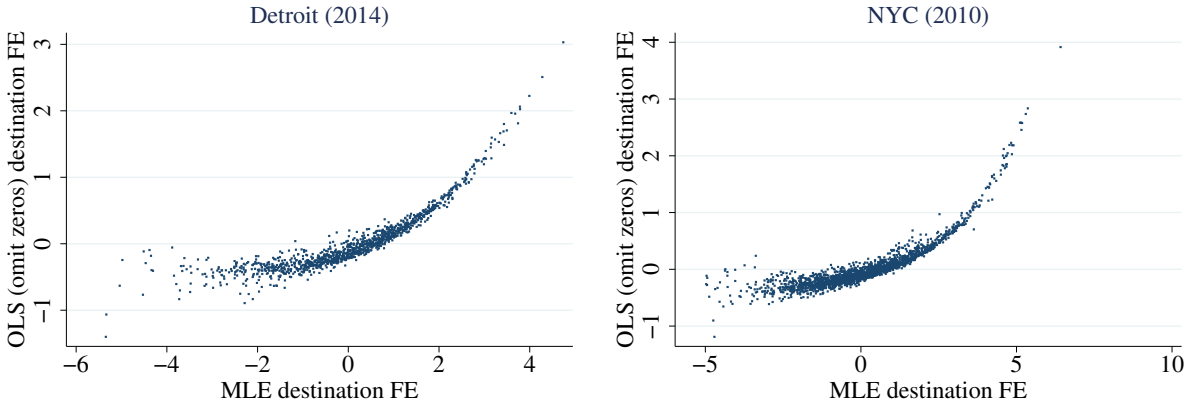

NOTES: These plots depict the destination fixed effects estimated in Table C.1's column 1 (horizontal axis) and column 3 (vertical axis). The left panel plots these fixed effects for Detroit; the right panel plots them for New York City. See the notes to Table C.1 for details.

Table C.2: Commuting elasticity estimates using distance for counties

	(1) MLE	(2) MLE non-zero	(3) OLS non-zero	(4) OLS recode
Commuting cost	-3.221	-3.064	-3.506	-20.31
	(0.0810)	(0.0778)	(0.0280)	(0.188)
Observations	79,112	42,687	42,687	79,128
Model fit (R^2 or pseudo-R^2)	0.927	0.917	0.765	0.564
Location pairs	79,188	42,785	42,785	79,188
Commuters	35,219,020	35,219,020	35,219,020	35,219,020

Standard errors, two-way clustered by k and n, in parentheses

NOTES: The estimation sample contains pairs of counties within 120 kilometers in the 2006–2010 ACS. All specifications include destination fixed effects and origin fixed effects. The covariate δ_{kn} is the geodesic distance between counties k and n. Column 1 presents the results from the maximum likelihood estimation described in Section 4.1.2. Column 2 presents the results from applying the maximum likelihood estimator to a sample that omits observations with zero commuters. Column 3 estimates the gravity equation in logs via OLS. Column 4 recodes $\ell_{kn} = 0$ observations to $\ell_{kn} = 10^{-12}\ell_{nn}$ before estimating the gravity equation in logs via OLS.

Figure C.2: Contrasting fixed effects from county-to-county gravity regressions

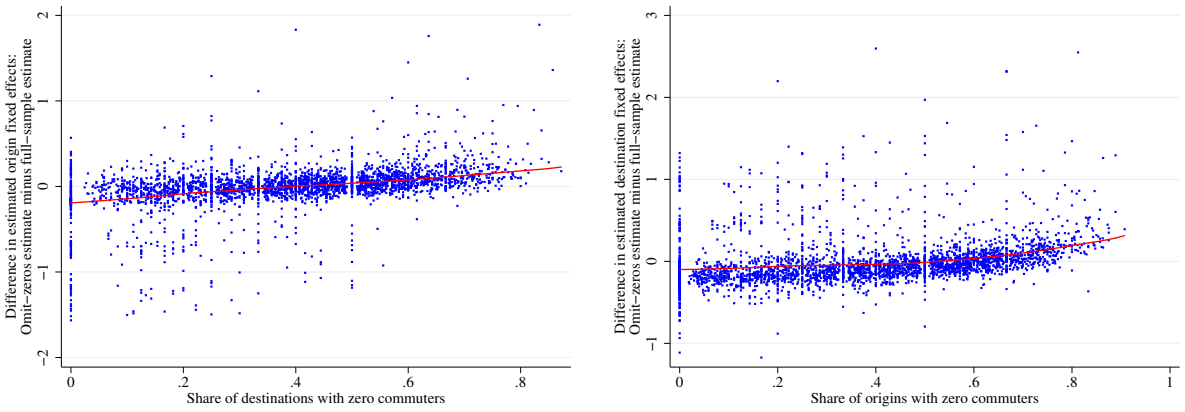

NOTES: These plots contrast county fixed effects estimated with and without zero-valued observations. The vertical axis of each panel is the difference between the fixed effect estimated when dropping zeros (Table C.2's column 2) and using the full sample (Table C.2's column 1). The horizontal axis of each panel is the share of observations for which there are zero commuters. The sample is all county pairs within 120 kilometers of each other in the 2006–2010 ACS. See Table C.2 notes for details on the estimation samples and estimators.

D Counterfactuals

D.1 Calibrated-shares procedure

This section describes a calibration procedure, known as "exact hat algebra" or "calibrated share form" in the international trade literature (Rutherford, 1995; Dekle, Eaton, and Kortum, 2008), often applied in quantitative spatial economics. This procedure makes a quantitative spatial model perfectly match the observed spatial distribution of economic outcomes and allows one to compute counterfactual equilibrium outcomes expressed as proportionate changes from the initial equilibrium.

The procedure relies on rewriting the equilibrium equations to describe ratios of counterfactual and initial equilibrium variables. To emulate the typical approach in the literature, we assume that commuting costs δ_{kn} are preference shifters rather than reduced labor hours. In this specification, the three equations that jointly define the equilibrium of the model in Section 3 when there is a continuum of individuals with continuum-case rational expectations, such that $\tilde{w}_n = w_n$ and $\tilde{r}_k = r_k$, are equation (6) and slight variants of equations (3) and (4):

$$
\begin{aligned}
A_n \sum_k \ell_{kn} &= \frac{(w_n/A_n)^{-\sigma}}{P^{1-\sigma}} \sum_{k',n'} \ell_{k'n'} w_{n'} \\
T_k &= \alpha \sum_n \ell_{kn} \frac{w_n}{r_k} \\
\ell_{kn} &= L \times \frac{w_n^{\epsilon} \left(r_k^{\alpha} \delta_{kn}\right)^{-\epsilon}}{\sum_{k',n'} w_{n'}^{\epsilon} \left(r_{k'}^{\alpha} \delta_{k'n'}\right)^{-\epsilon}}.
\end{aligned}
$$

The researcher knows the labor demand elasticity σ and commuting elasticity ϵ and observes the initial equilibrium labor allocation ℓ_{kn} and wages w_n. Denote counterfactual equilibrium values of wages, rents, and labor allocation by w'_n, r'_k, and ℓ'_{kn}. Denote the counterfactual-initial ratio of a variable x by $\hat{x} \equiv \frac{x'}{x}$. Assume that $\ell'_{kn} = 0$ if $\ell_{kn} = 0$, so that, in a slight abuse of notation, we can write $\hat{\ell}_{kn} = 1$ if $\ell_{kn} = 0$.

One can solve for the counterfactual equilibrium variables associated with combinations of counterfactual-initial ratios of productivities $\hat{A}_n$, land endowments $\hat{T}_k$, and commuting costs $\hat{\delta}_{kn}$. Tedious manipulation of the three equations above leads to the following three equations written

in terms of elasticities, initial equilibrium values, and counterfactual-initial ratios:

$$\hat{w}_n = \hat{A}_n^{\frac{\sigma-1}{\sigma}} \left(\sum_n \left(\frac{\hat{w}_n}{\hat{A}_n} \right)^{1-\sigma} \frac{w_n \sum_k \ell_{kn}}{\sum_{k',n'} w_{n'} \ell_{k'n'}} \right)^{\frac{-1}{\sigma}} \left(\frac{\sum_k \hat{\ell}_{kn} \ell_{kn}}{\sum_k \ell_{kn}} \right)^{\frac{-1}{\sigma}} \left(\sum_{k',n'} \frac{\hat{\ell}_{k'n'} \ell_{k'n'} \hat{w}_{n'} w_{n'}}{\sum_{k',n'} \ell_{k'n'} w_{n'}} \right)^{\frac{1}{\sigma}} \tag{D.1}$$

$$\hat{r}_k = \hat{T}_k^{-1} \sum_n \frac{\hat{\ell}_{kn} \ell_{kn} \hat{w}_n w_n}{\sum_n \ell_{kn} w_n} \tag{D.2}$$

$$\hat{\ell}_{kn} = \begin{cases} 1, \text{ if } \ell_{kn} = 0 \\ \dfrac{\hat{w}_n^{\varepsilon} (\hat{r}_k^{\alpha} \hat{\delta}_{kn})^{-\varepsilon}}{\sum_{k',n'} \hat{w}_{n'}^{\varepsilon} \hat{r}_{k'}^{-\alpha\varepsilon} \hat{\delta}_{k'n'}^{-\varepsilon} \frac{\ell_{kn}}{L}}, \text{ if } \ell_{kn} > 0 \end{cases} \tag{D.3}$$

These three equations deliver $\hat{w}_n$, $\hat{r}_k$, and $\hat{\ell}_{kn}$ given the elasticities σ and ϵ, initial equilibrium values ℓ_{kn} and w_n, and counterfactual-initial ratios $\hat{A}_n$, $\hat{T}_k$, and $\hat{\delta}_{kn}$.

Note that this procedure implicitly rationalizes zero-commuters observations with infinity commuting costs, $\ell_{kn} = 0 \iff \delta_{kn} = \infty$. This procedure cannot characterize cases in which $\ell_{kn} = 0$ and $\ell'_{kn} \neq 0$ because the object $\hat{\delta}_{kn}^{-\epsilon} = \left(\frac{\delta'_{kn}}{\delta_{kn}} \right)^{-\epsilon}$ is not sensibly defined if $\delta'_{kn} \neq 0$ and $\delta_{kn} = \infty$.

Note that this procedure does not identify the initial values of the parameters A_n, T_k, and δ_{kn}. Given the elasticities σ and ϵ and the initial equilibrium values ℓ_{kn} and w_n, equations (3), (4), and (6) are insufficient to separately identify T_k and δ_{kn}. One would also need to observe land prices r_k to separate these parameters.

When implementing this procedure in Section 5, we compute tract-level workplace wages using LODES and ZIP Business Patterns data following Owens, Rossi-Hansberg, and Sarte (2020).

D.2 Event studies

Figure D.1 depicts the time series of total employment in two New York City census tracts that contain 200 Fifth Avenue and 111 Eighth Avenue. In Section 5, we examine tract-to-tract commuting flows within New York City for which these two tracts are workplaces (commuting destinations).

D.3 Monte Carlo exercise

A Monte Carlo exercise shows that granularity alone can substantially reduce the predictive power of the calibrated-shares procedure. In this simulation, the data-generating process is our estimated model of New York City in 2010. We impose a counterfactual 18% increase in productivity for the tract containing 200 Fifth Avenue. In the limiting case, as $I \to \infty$, the calibrated-shares procedure would perfectly describe the changes in commuting flows associated with this productivity increase. Thus, any predictive failure when drawing granular ($I = 2,488,905$) realizations from this data-generating process are due to problems stemming from the "continuum of individuals" assumption.

Given our estimated model of New York City in 2010, we simulate 100 "event studies" as in Section 5. For each of the 100 events, we implement the following five steps:

1. To mimic "observed" data, draw one realization from the data-generating process at its 2010 parameter values and one realization at its counterfactual parameter values. Compute the difference in employment in the tract containing 200 Fifth Avenue.

2. Estimate the granular model and calibrate the continuum model to match the realization drawn from the data-generating process at its 2010 parameter values.

3. Compute the increase in productivity required to match the "observed" change in employment for the "treated" tract for both the calibrated-shares procedure and the granular model. These increases may differ from each other and the true 18% increase.

4. Compute the predicted change in commuter counts for the calibrated-shares procedure and 1,000 simulations of the granular model.

5. Regress the "observed" changes in commuter counts destined for the tract containing 200 Fifth Avenue on the calibrated-shares predicted changes. Regress the "observed" changes in commuter counts destined for the tract containing 200 Fifth Avenue on the mean of the predicted changes from 1,000 granular simulations.

We summarize the 100 simulations by plotting the coefficients and relative RMSEs in Figure D.2, which is analogous to Figure 6 in Section 5.

The Monte Carlo simulation shows that our estimation procedure recovers model parameters well enough when the granular model is the data-generating process to predict counterfactual changes in commuter counts. By contrast, the calibrated-shares procedure has limited predictive power when applied to granular data. Figure D.2 shows that regressing the "observed" changes in commuter counts on the values predicted by the calibrated-shares procedure yields a slope that is close to zero and an intercept that is far from it. Since the only element of the data-generating process at odds with the assumptions of the calibrated-shares procedure is the finite number of individuals, granularity alone can severely limit that procedure's predictive power.

Figure D.1: Employment increases in the anchor-tenant event-study tracts

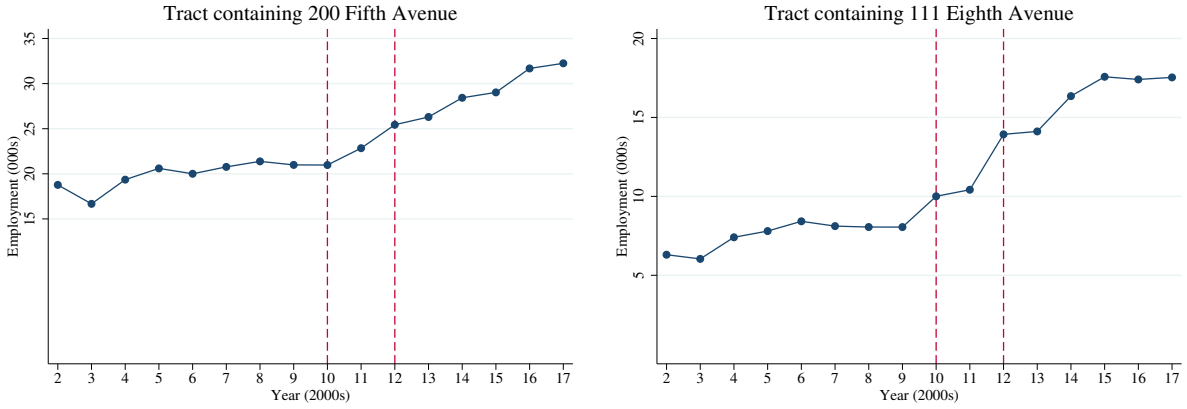

NOTES: This figure depicts the number of primary jobs in tracts 36061005800 and 36061008300 in the LODES data.

Figure D.2: Monte Carlo: Calibrated-shares procedure performs poorly with granular data